Journal of Materials Chemistry A

ROYAL SOCIETY OF CHEMISTRY

REVIEW

View Article Online
View Journal | View Issue

Cite this: *J. Mater. Chem. A*, 2025, **13**, 12785

Benzodithiophene-based polymer donors for organic photovoltaics

Meng Wei and Dmytro F. Perepichka *

Received 1st October 2024
Accepted 16th March 2025

DOI: 10.1039/d4ta07020h

rsc.li/materials-a

The advancement of π-conjugated polymers has contributed to the rapid development of high-performing organic photovoltaic (OPV) devices. The donor (D)–acceptor (A) conjugated polymers dominated the field of OPV materials as these structures offer opportunities to fine-tune material properties such as bandgap, charge transport and solubility. Among all the D building blocks, benzodithiophene (BDT) has received extensive attention owing to its symmetric structure, convenient attachment points for side chains and high stability. This review summarizes the general molecular design strategy for BDT-based D–A copolymers and gives carefully selected examples of such copolymers used in NFA solar cells, aiming to provide a structure–property relationship for rational design of future BDT-based D–A conjugated polymers.

Introduction

Organic photovoltaic (OPV) technology is emerging as one of the promising pathways to transform solar energy into electricity. Compared to conventional solar cells based on silicon and other inorganic semiconductors, OPVs bring several advantages such as flexibility, light weight, low CO_2 footprint of fabrication and the possibility of mass production through printing.

The first demonstration in OPV diodes based on the planar (bilayer) heterojunction of copper phthalocyanine and a perylenediimide derivative was reported by Tang in 1986, achieving a power conversion efficiency (PCE) of ~1%.[1] The current generation in this device was limited by inefficient exciton dissociation away from the donor/acceptor interface (Fig. 1). The invention of the bulk-heterojunction (BHJ) OPV in 1995[2,3] addressed this problem by providing an active layer of interpenetrated p-/n-type domains by blending the conjugated poly(2-methoxy-5-(2′-ethylhexyloxy)-1,4-phenylenevinylene) (MEH-PPV, Fig. 2) donor with a derivatized fullerene ($PC_{61}BM$) acceptor. Polymer-based OPVs have since dominated the field. Other homopolymers such as poly(3-hexylthiophene) (P3HT) were introduced in OPV devices and a PCE of 5% has been achieved with P3HT around 2007.[4–6]

The relatively large band-gap (E_g) of homopolymers (~2.2 eV for MEH-PPV, ~2.0 eV for regioregular P3HT) leaves unconverted a significant portion of solar radiation which peaks at around 700 nm (1.77 eV). To address this problem, low bandgap donor–acceptor (D–A) copolymers were developed and eventually became dominant in the OPV field. The orbital mixing in a chain of alternating electron-rich D and electron-deficient A moieties results in E_g contraction (Fig. 3) and redshift of the absorption band.[7] Also, as established later, quadrupole interactions between the polarized chains of D–A copolymers lead to stronger interchain coupling increasing the charge mobility. The period between 2008 and 2015 witnessed a rapid development of low bandgap D–A copolymers such as PTB7 and OPV devices based on D–A polymer/fullerene blends reached a PCE of ~12%. With the recent rise of non-fullerene acceptors (NFA), which can strongly absorb in the visible and NIR regions,[8] the requirements for donor polymers have slightly changed, and nowadays they are engineered to present a relatively wide E_g with an absorption profile complementary to NFA molecules (*e.g.*, PM6).

Various donor units, such as cyclopentadithiophene and carbazole, have been used as building blocks for conjugated polymers.[9–11] Among these, benzo[1,2-*b*:4,5-*b*′]dithiophene (BDT) has proved to be particularly versatile and most of the highest efficiency OPVs nowadays employ BDT-containing

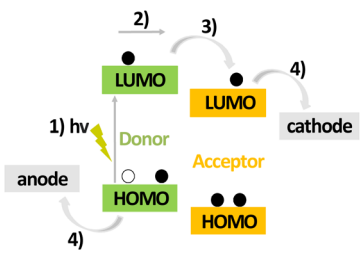

Fig. 1 Operation of OPVs: (1) absorption of light and generation of an exciton; (2) diffusion of the exciton to the donor–acceptor interface; (3) exciton dissociation and charge separation at the interface; (4) free charge carrier transport and extraction on electrodes.

Department of Chemistry, McGill University, 845 Sherbrooke St W, Montreal, Quebec H3A 0G4, Canada. E-mail: dmytro.perepichka@mcgill.ca

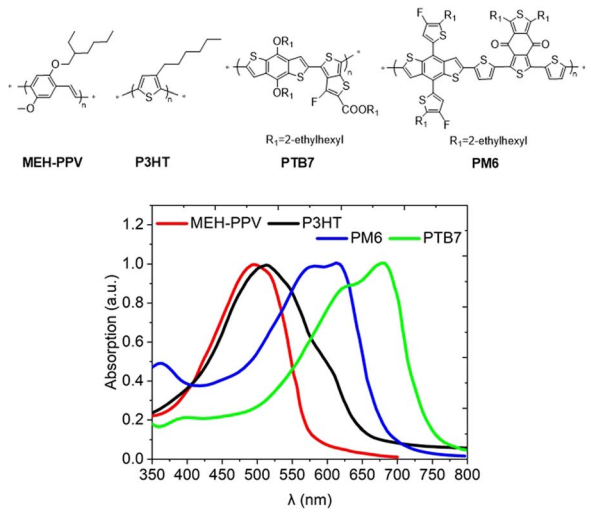

Fig. 2 Solid state UV-vis absorption spectra of MEH-PPV, P3HT, PM6 and PTB7 polymers used in OPVs.

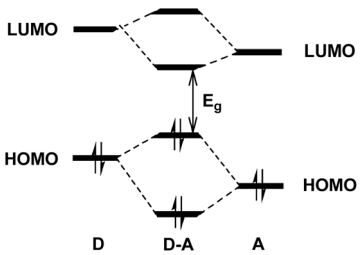

Fig. 3 Molecular orbital interactions of the donor and acceptor, resulting in a narrowing of the band gap in D–A copolymers.

polymers as donor materials. There are several reasons for this choice. BDT has a symmetric rigid planar structure with a 180° angle between the connection sites, resulting in a linear polymer structure with efficient stacking as well as excellent thermal and chemical stability. Solubilizing chains can be installed on the benzene ring of BDT without affecting the planarity of the conjugated backbone (unlike many other thiophene-based polymers including P3HT[12]).

BDT monomers were reported for the first time in 1971 (ref. 13) and incorporated in conjugated polymers in the 1990s.[14] In 2008, D–A copolymers of BDT with various acceptors were used for the first time in OPVs.[15]

The development of D–A conjugated polymers for organic solar cells has been extensively reviewed in the past with various focuses, with BDT-containing copolymers also being covered.[16–20] The most comprehensive review focused on BDT polymers was published in 2016,[21–24] before the recent wave of research in OPVs with NFAs. Several recent reviews have discussed the design and application of BDT polymers in combination with NFAs in BHJ solar cells.[25,26] Nevertheless, the continuous and rapid development of the field of OPVs creates a need for an up-to-date review putting the most recent contributions in the perspective of milestone discoveries of the past.

The present paper summarizes the most up-to-date literature to provide the current design principles and structure–property relationship studied in BDT-based D–A conjugated polymers in the context of their applications in OPVs. After a brief introduction to the synthesis of BDT monomers and polymerization approaches, we summarize the main design strategies in engineering their electronic properties, including main-chain engineering and side-chain engineering. We then review key examples of wide bandgap BDT-based polymer donors that are used in combination with NFAs in OPVs. Lastly, we provide an outlook for the remaining challenges and future perspectives in BDT-based polymer materials. Without the intention of comprehensive coverage of all literature on BDT-based polymers, we hope this paper will provide a fair and rounded overview of the recent advances in the field and opportunities for future development.

Synthesis of the BDT monomer and BDT-based polymers

BDT monomers are most commonly synthesized starting from 3-thiophenecarboxamide **M1** through lithiation at the 2-position followed by intermolecular cyclization with another molecule of **M1** (Scheme 1). The resulting diketone **M2** can be reductively aromatized with the addition of solubilizing side groups on the central benzene ring. The alkoxy-substituted BDTs **M3** are typically synthesized by first reducing the keto-groups in **M2** to the diol intermediate, followed by alkylation with alkyl halide. Alkylthio-substituted BDTs **M4** can be accessed by esterifying the diol with *N*,*N*-dimethylthiocarbamoyl chloride followed by rearrangement and cleavage of the resulting thiocarbamate, and alkylation of the formed dithiol intermediate.[27,28] Reacting **M2** with aryllithium reagent yields the corresponding diol intermediate which can be reductively aromatized using $SnCl_2$ to afford aryl-substituted monomer **M5**. Replacing the aryllithium with alkynyllithium results in the alkynyl-flanked BDT **M6**. Its hydrogenation on Pd/C produces alkyl-substituted BDT **M7**,[29] which can also be made directly by reacting **M2** with alkyllithium followed by $SnCl_2$ reduction.[30] BDT flanked with asymmetric side chains **M8** can also be synthesized by stepwise monoarylation, reduction and alkylation.[31]

The most common method for the synthesis of D–A copolymers is Pd-catalysed Stille coupling between distannylated and dibrominated monomers (Scheme 1c). Typically, trimethyl or tributyltin functionalized BDTs (prepared *via* a lithiation-stannylation sequence) are cross-coupled with dihalogenated acceptor units. In some cases, Stille polymerization of dibromo-BDT derivatives has also been reported.[32] The versatility of Stille coupling in the synthesis of thiophene-based polymers makes it a method of choice most of the time. Indeed, it remains the most reliable method used in commercial production of benchmark BDT polymers such as **PM6** (polymer **51**) and **D18** (polymer **75**).

However, it also has multiple drawbacks, including the formation of stoichiometric amounts of toxic tin byproduct and the limited shelf-life of tinylated monomers explaining the

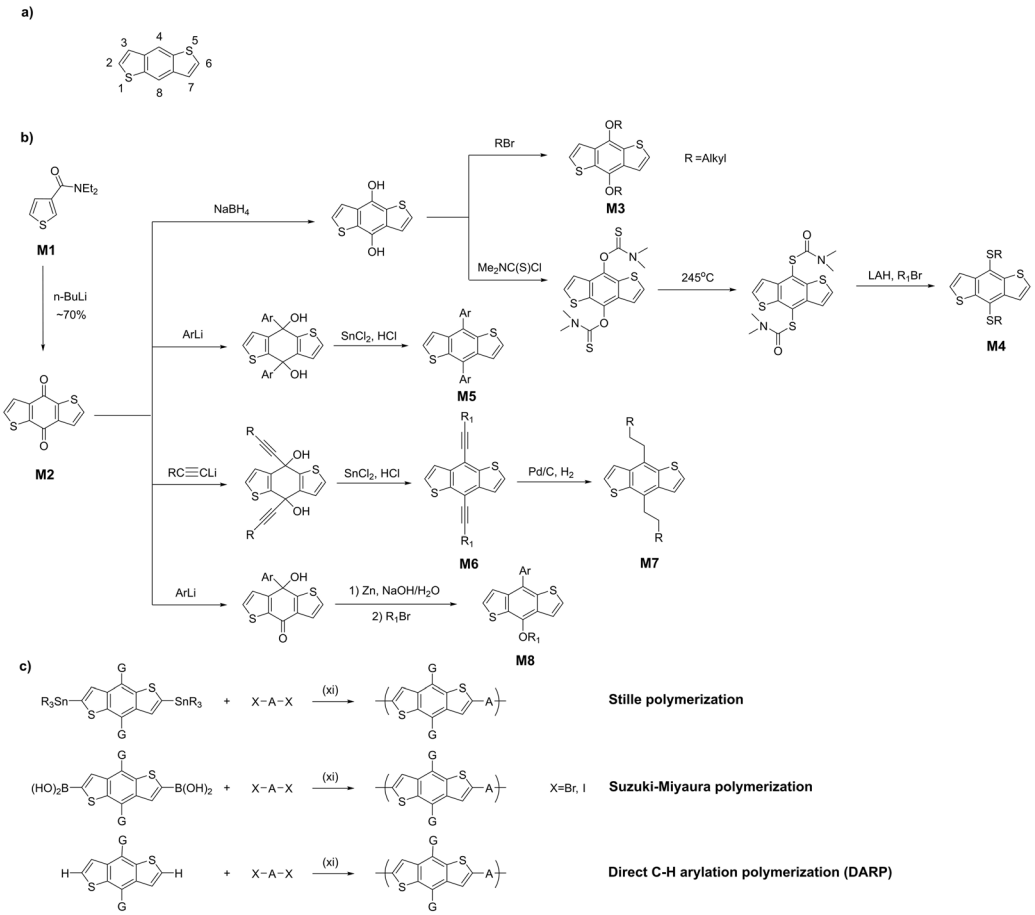

Scheme 1 Numbering of BDT (a) and synthesis of (b) BDT monomers and (c) BDT-based polymers.

interest in exploring alternative polymerization methods, especially for large-scale synthesis.

The application of more benign Suzuki–Miyaura in the thiophene series is often limited by the instability of the corresponding boronic acid monomer under reaction conditions.[33] As a result, it is rarely employed in the synthesis of BDT polymers. One notable exception is the work of Xiao *et al.* who synthesized new BDT monomers and polymerized their dihalides with acceptors equipped with boronic acid groups.[34] It is worth noting that in this case, 0.5 h reaction time was sufficient to produce a polymer with a molecular weight of nearly 30 000 g mol^{-1}, indicating the efficacy of the Suzuki reaction.[35]

Direct C–H arylation polymerization (DArP) is gaining increasing attention in the synthesis of D–A copolymers. This method generates mild byproducts (alkali metal halide) and eliminates the pre-functionalization (stannylation/borylation) step resulting in an overall significant cost reduction compared to the classical cross-coupling reactions.[36] The early work on DArP of dibromo-BDT[37] with various aromatic comonomers showed high (75–95%) yields of copolymers with similar polydispersities and molecular weights rivalling or exceeding those of reference copolymers synthesized *via* Stille coupling. Moreover, this study reveals comparable or superior photovoltaic properties *versus* the same polymers made by Stille coupling, for the first time reaching a PCE of 8% for a DArP-produced material. It should be noted that the presence of different aromatic C–H bonds in comonomers intrinsically limits the regioselectivity of DArP compared to Stille or Suzuki polymerization.[37–39] In this context, BDT is well suited for DArP because the steric hindrance of the β-CH makes it significantly less reactive than the α-CH. However, an appropriate choice of arenedibromide comonomer and optimization of polymerization conditions is required to minimize the homocoupling defects in the resulting copolymer.[40–42]

Regardless of the polymerization methods, batch-to-batch variability[43] is a major concern for commercial applications of BDT (and other) conjugated polymers in OPVs. This variability originates from several factors, including molecular weight and polydispersity (chain length distribution), side reactions during synthesis such as homocoupling, remaining traces of catalytic metal, *etc.*[44] A few aspects need to be considered to minimize this problem for existing polymers, including type of catalyst and ligand, reaction setup, *etc.* For example, replacing the standard $Pd(PPh_3)_4/Pd_2(dba)_3$ with commercial Buchwald catalyst ($P(tBu)_3Pd$ G3) allows reducing homocoupling defects in **PM6** below the detection level.[45] Another promising approach to combat the batch-to-batch variability is flow synthesis which was recently used to produce **PM6** with controlled molecular weights

and reproducible device performance.[45] Last but not least, the monomer purity and post-treatment (*e.g.* Soxhlet extraction) of the crude polymer play a critical role in reducing batch-to-batch variations.[46]

Molecular design strategy of BDT-based conjugated polymers for OPVs

One of the major properties of interest in OPV donors is their bandgaps. There are multiple factors that influence the bandgap of a conjugated polymer: bond-length alternation, aromaticity, planarity and the electronic effect of substituents.[47] Another important feature is charge mobility, which depends on conjugation within the chain as well as the packing of polymer chains. Last but not least, the solubility and processability of a polymer in green solvents matter when the material is fabricated into the device, especially when it comes to the commercialization stage. All these properties can be fine-tuned *via* careful engineering of the polymer backbone (main chain) and substituents (side chains).

Main-chain engineering

Donor–acceptor approach. In 2008, Hou, Yang and co-workers reported a series of BDT-based copolymers **1–8** (Fig. 4 and Table 1) with controlled bandgap.[15] As shown in Table 1, λ_{max} of all the copolymers have a redshifted absorption compared to homopolymer **1**, and copolymer **8** with the most electron-deficient thienopyrazine unit displays a redshift as large as 285 nm. The bandgaps of polymers **1–8** vary between 1.1 and 2.1 eV and the highest occupied molecular orbital (HOMO) level is tuned between −4.6 eV and −5.2 eV. This study demonstrated the versatility of BDT polymers in the design of conjugated polymers with controlled bandgap and energy levels, and showed their first application in OPV devices, albeit with low efficiency (PCE ≤ 1.6%).

Since then, a number of acceptor units have been copolymerized with BDT to develop donor polymers for OPVs. Early examples include diketopyrrolopyrrole (DPP) (polymer **9**)[48] and thieno[3,4-*b*]thiophene (TT) carboxylic ester (polymer **10**)[49] moieties (Fig. 5). In 2009, a PCE of 5.3% was achieved with a **10** : $PC_{71}BM$ blend, demonstrating the potential of D–A copolymers as alternatives to homopolymers for OPV applications (Table 2).

Table 1 Absorption maxima and the bandgap of polymers **1–8** in films and corresponding HOMO/LUMO energies obtained by cyclic voltammetry

	λ_{max} (nm)	E_g (eV)	HOMO (eV)	LUMO (eV)
1	495	2.13	−5.16	−2.67
2	511	2.06	−5.05	−2.69
3	510	2.03	−5.07	−2.86
4	532	1.97	−4.56	−2.66
5	591	1.7	−5.1	−3.19
6	601	1.63	−4.78	−3.28
7	641	1.52	−4.88	−3.33
8	780	1.05	−4.65	−3.46

A strong electron-withdrawing benzo[*c*][1,2,5]thiadiazole (BT) unit connected *via* a thiophene bridge was incorporated in copolymer **11**.[50] This combination results in a rather low HOMO of −5.26 eV (*cf.* −5.16 eV for DPP copolymer **9**), contributing to a relatively high open-circuit voltage (V_{OC}) of 0.76 V for the **11** : $PC_{61}BM$ solar cell. Replacing benzothiadiazole with a benzoselenadiazole acceptor presents a further reduction of the bandgap from 1.70 for **11** to 1.55 eV for **12** and a PCE of 5.2% was obtained for **12** : $PC_{71}BM$ blends.[51]

Conversely, replacing sulfur in the BT unit with electron-donating nitrogen results in a weaker benzo[*d*][1,2,3]triazole (BTz) acceptor, which is beneficial for developing wider bandgap polymers. The additional alkyl chains on the nitrogen atom provide an additional handle to tune the solubility and packing of BTz-containing polymers. However, polymer **13** bearing a BTz acceptor displays a wider bandgap (1.95 eV) with blue-shifted absorption by over 100 nm compared to its BT counterpart **11**.[52] Furthermore, the high-lying HOMO of −5.06 eV of **13** results in a lower V_{OC} of 0.61 V and a PCE of only 1.5% for the BHJ with $PC_{61}BM$.

Another acceptor that gained significant attention is benzo[1,2-*c*:4,5-*c*′]dithiophene-4,8-dione (BDD).[20] The first polymer with alternating alkoxy-substituted BDT and BDD was reported in 2012, but the PCE of the corresponding devices was low (0.7% with $PC_{71}BM$).[53] A few months later, a similar polymer **14** (commonly known as **PBDB-T**) consisting of an alkylthienyl-substituted BDT unit and BDD with thiophene as π-linkers was reported.[54] This polymer has a HOMO of −5.23 eV and its device with $PC_{61}BM$ delivered a relatively high V_{OC} of 0.86 V with

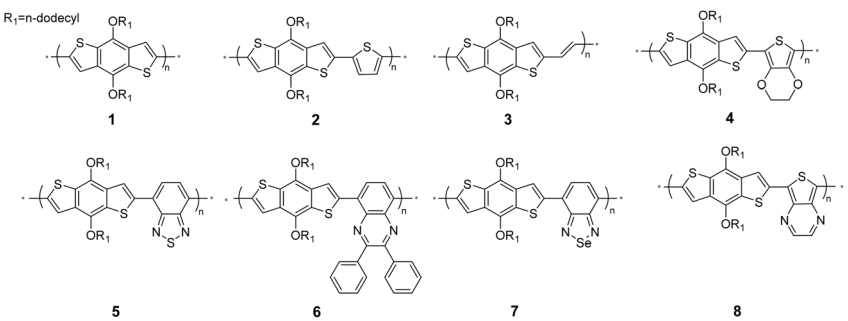

Fig. 4 Conjugated copolymers **1–8** based on BDT and varied acceptor units.

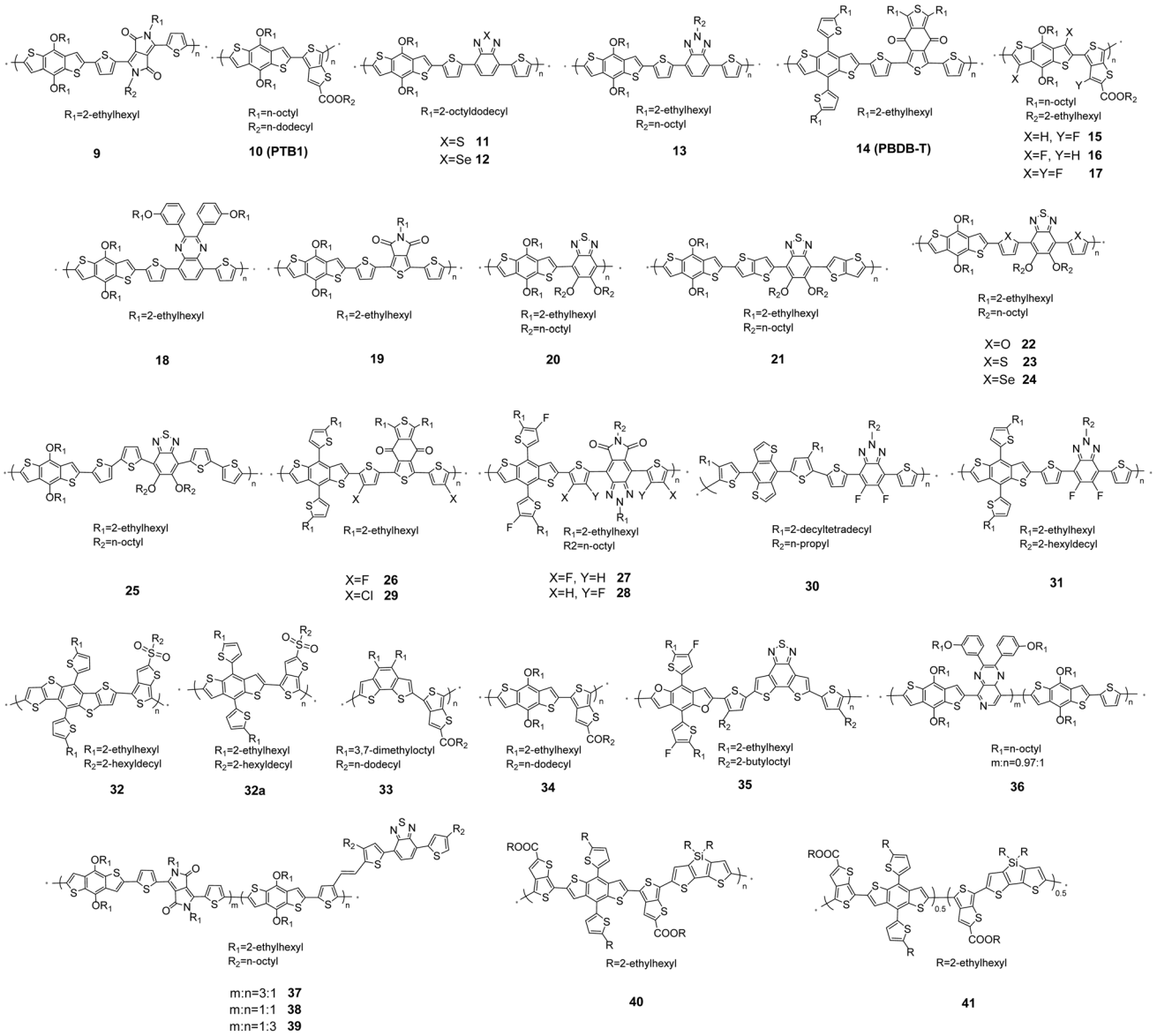

Fig. 5 Main chain engineering in D–A copolymers **9–41**.

a PCE of 6.7%. Notably, **14** displays a temperature-dependent aggregation behavior in solution. This behavior enables the control of polymer pre-aggregation before casting the films, leading to a favorable morphology and improving the device performance.[55]

Fluorination is an extensively studied strategy for tuning the properties of conjugated polymers. Due to the high electronegativity and small size, fluorine effectively lowers the HOMO and LUMO energies of the material without inflicting steric hindrance and twisting the polymer structure. Furthermore, it can planarize/rigidify the polymer backbone through intramolecular F···H and F···S interactions. The effect of the number and position of fluorine substituents has been explored in the series of polymers **15–17**.[56] Increasing the number of fluorine atoms results in progressive stabilization of its frontier orbitals, by up to 0.5 eV, as well as an increased planarity of the backbone (due to intramolecular S···F interactions). However, the fluorination on BDT decreases its electron-donating ability, resulting in a wider bandgap of polymer **16** (1.75 eV) compared to **15** with a fluorinated acceptor (1.68 eV). The devices with **15** and $PC_{71}BM$ yielded a PCE of up to 7.2%, a significant improvement *vs.* non-fluorinated analog **10** (5.3%). On the other hand, polymers **16** and **17**, which use fluorinated BDT units, showed poor device performance (PCE 3.2% and 2.7%) due to excessive phase separation of the highly fluorinated donor and $PC_{71}BM$ acceptor.

Other prominent examples include BDT copolymers with quinoxaline (**18**,[57]) and thiophenedicarboximide (**19**,[58]) acceptor units.

Additional π-linkers. Additional π-linkers are often introduced between BDT and acceptor units to reduce the steric repulsion and twisting of the polymer chain. Commonly studied

Table 2 Optical, electronic, and photovoltaic performances of **9–41**

	Polymer properties				OPV device						
	λ_{max}[a] (nm)	E_g^{opt}[a] (eV)	HOMO[b] (eV)	LUMO[b] (eV)	wt/wt (acceptor)	V_{OC} (V)	J_{SC} (mA cm^{-2})	FF (%)	PCE (%)	Ref.	Year of report
9	750	1.31	−5.16	−3.51	1 : 1 ($PC_{71}BM$)	0.68	8.4	44.3	2.5	48	2009
10	690	1.62	−4.9	−3.2	1 : 2 ($PC_{71}BM$)	0.56	15	63.3	5.3	49	2009
11	646	1.7	−5.26	—	1 : 1 ($PC_{61}BM$)	0.76	8	64.4	3.9	50	2013
12	680	1.55	−5.18	−3.48	1 : 1 ($PC_{71}BM$)	0.6	13.6	64	5.2	51	2013
13	527	1.95	−5.06	−3.11	1 : 3 ($PC_{61}BM$)	0.61	4.4	55	1.5	52	2010
14	622	2.05(E_g^{EC})	−5.23	−3.18	1 : 1 ($PC_{61}BM$)	0.86	10.7	72.3	6.7	54	2012
15	671	1.68	−5.15	−3.31	1 : 1.5 ($PC_{71}BM$)	0.74	14.1	68.9	7.2	56	2011
16	670	1.75	−5.41	−3.6	1 : 1.5 ($PC_{71}BM$)	0.68	11.1	42.2	3.2	56	2011
17	670	1.73	−5.48	−3.59	1 : 1.5 ($PC_{71}BM$)	0.75	9.1	39.4	2.7	56	2011
18	602	1.74	−5.12	−3.38	1 : 2 ($PC_{71}BM$)	0.71	7	61.5	3.1	57	2012
19	516	1.84	−5.49	−3.7	1 : 2 ($PC_{61}BM$)	0.76	2.9	43	1.0	58	2011
20	620	1.69	−5.17	−3.49	1 : 2 ($PC_{71}BM$)	0.66	1.8	41.8	0.5	60	2012
21	631	1.78	−5.21	−3.54	1 : 1.5 ($PC_{71}BM$)	0.69	11.3	63	4.9	59	2012
22	534	1.96	−5.44	−3.48	1 : 2 ($PC_{71}BM$)	0.94	6.5	46	2.8	59	2012
23	568	1.82	−5.35	−3.44	1 : 1.5 ($PC_{71}BM$)	0.82	9.5	48	3.7	59	2012
24	644	1.71	−5.29	−3.33	1 : 2 ($PC_{61}BM$)	0.65	8.6	54.5	3.1	61	2012
25	575	1.8	−5.37	−3.01	1 : 2 ($PC_{71}BM$)	0.66	13.3	58.1	5.1	62	2015
26	644	—	−5.47	−3.46	1 : 1.25 (C8-ITIC)	0.94	19.6	72.0	13.2	63	2018
27	642	1.72	−5.55	−3.83	1 : 1 (Y6)	0.85	26.3	75.5	16.8	64	2020
28	505	2.09	−5.67	−3.58	1 : 1 (Y6)	0.80	4.9	36.5	1.4	64	2020
29	647	1.78	−5.48	−3.47	1.2 : 1 (IT-4F)	0.84	20.6	71.1	12.3	65	2018
30	—	2.05	−5.47	−3.42	1 : 1.5 (o-IDTBR)	1.08	16.3	63.6	11.6	66	2017
31	538	1.96	−5.21	−2.99	1 : 1 (ITIC)	0.73	13.1	57.8	5.5	67	2016
32	778	1.59	−5.21	−1.08	1 : 1.5 ($PC_{71}BM$)	0.73	16.6	64.1	7.8	68	2013
32a	768	1.61	−5.29	−1.00	1 : 1.5 ($PC_{71}BM$)	0.81	11.8	52.1	5.0	68	2013
33	662	1.55	−5.35	−3.80	1 : 2 ($PC_{71}BM$)	0.82	11.8	54.1	5.2	70	2011
34	—	1.61	−5.12	−3.55	1 : 1.5 ($PC_{71}BM$)	0.70	14.7	64	6.6	71	2009
35	588	1.97	−5.48	−3.42	1 : 1.2 : 0.2 (Y6-1O : $PC_{71}BM$)	0.90	23.62	80.4	17.1	72	2022
36	634	1.6	−5.2	−3.28	1 : 4 ($PC_{71}BM$)	0.71	6.4	51.7	2.4	74	2010
37	746	1.43	−5.29	−3.7	1 : 2 ($PC_{61}BM$)	0.72	6.2	49.0	2.2	75	2014
38	734	1.47	−5.36	−3.69	1 : 2 ($PC_{61}BM$)	0.74	12.2	46.0	4.2	75	2014
39	723	1.52	−5.47	−3.67	1 : 2 ($PC_{61}BM$)	0.78	14.1	48.0	5.3	75	2014
40	691	1.45	−5.19	−3.62	1 : 1.5 ($PC_{71}BM$)	0.64	14.4	61.8	5.6	76	2016
41	649	1.28	−5.08	−3.62	1 : 1.5 ($PC_{71}BM$)	0.50	5.6	39.2	1.1	76	2016

[a] In thin films, bandgap derived from absorption onset. [b] Measured with cyclic voltammetry.

π-linkers include single rings such as thiophene, furan, and selenophene, as well as multiple or fused rings such as bithiophene and thienothiophene. The hole mobility of **23** which bears a thiophene π-linker between BDT and BT units[59] is an order of magnitude higher than that of the analog **20** without the linker,[60] suggesting a more ordered packing of the polymer chains in **23**.

Changing the π-linker from furan (**22**) to thiophene (**23**) to thienothiophene (**21**) increases the angle between the two bonds connecting the π-bridge with the other moieties (127°, 152°, and 180°, respectively) and leads to a better packing of the more linear chains of **21**.[59] **21** has redshifted film absorption and reduced bandgap compared to **22** and **23**. It is also worth noting that **21–23** all showed better planarity and higher hole mobility than polymer **20** without such linkers. Changing heteroatoms in the π-linker from oxygen to sulfur to selenium results in redshifted absorption (lower bandgap) and increased HOMO energies (**22** *vs.* **23** *vs.* **24**).[59,61] The relatively low HOMO level of **22** resulted in a high V_{OC} of 0.94 V in OPV with $PC_{71}BM$. Fusing the π-linker enhances the backbone planarity which is manifested in a ∼60 nm red shift of thienothiophene polymer **21** compared to bithiophene polymer **25**.[62]

Fluorinating the thiophene π-linker in **26** (ref. 63) stabilizes the HOMO levels of **26** by ∼0.25 eV compared to **14** which leads to a high V_{OC} of 0.94 V and PCE of 13.2% (in the BHJ with NFA **C8-ITIC**, Fig. 6). It is worth noting that the position of the fluorine on the π-linker can affect the molecular conformation, aggregation morphology, and the optoelectronic properties of the polymer. **27** with fluorine proximal to the BDT unit exhibits an almost flat backbone, while its isomer **28** has a 42° twist between the acceptor and π-bridge.[64] This difference leads to a ∼100 nm redshift of absorption and a narrower bandgap of 0.37 eV in **27** which is responsible for its high PCE of 16.8% when used with acceptor **Y6** (Fig. 6).

The chlorinated thiophene π-linker in **29** affords similar energy levels and band-gap to those of fluorinated analog **26**, indicating the backbone planarity was not disturbed by the larger chlorine atoms.[65] It should be noted, though, that the position of chlorine on the π-linker can significantly influence

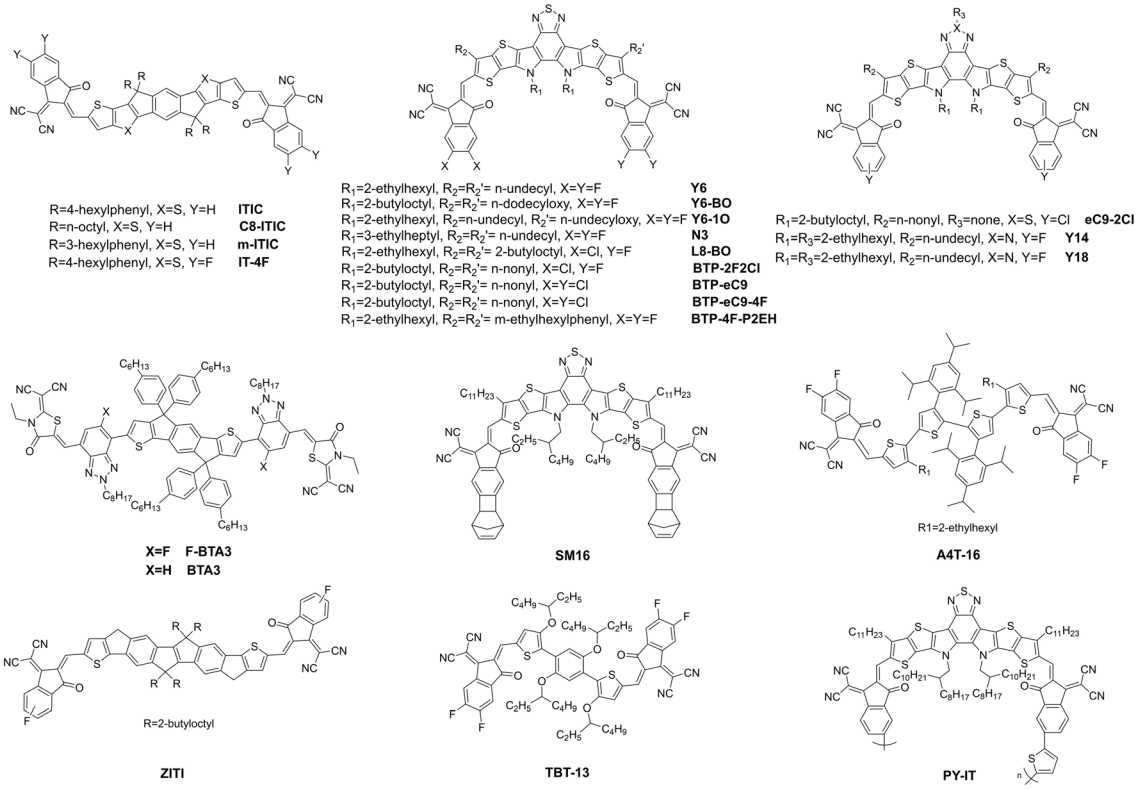

Fig. 6 Non-fullerene acceptors (NFAs) discussed in this paper.

the optoelectronic properties and photovoltaic performance of the polymer.[65]

Variations of BDT structure. The basic structure/connectivity of the benzodithiophene with two substituents in 4,8-positions and linked in the chain through 2,6-positions (Scheme 1a) has certainly been the most successful in the design of conjugated polymers. However, other variations have also been explored. BDT units were connected in the polymer chain *via* 4,8-positions in polymer **30**, and such connectivity reduced the planarity of the polymer backbone.[66] As a result, **30** displays a larger bandgap (2.05 eV) compared with its analog **31** (1.96 eV)[67] with common 2,6-connectivity. Despite its twisted backbone, polymer **30** provides a reasonable hole mobility (7×10^{-4} cm^2 V^{-1} s^{-1}) and a decent PCE of 11.6% was reported in blends with NFA o-IDTBR.[62] The 2,6-positions in this polymer **30** were unsubstituted (and potentially vulnerable to cross-coupling in the device). However, these sites allow the π-conjugation to be extended in the second direction (orthogonal to the main chains by attaching aromatic substituents, see the Extending side chain conjugation section below), which could be a subject for further polymer design efforts.

Two extra thiophenes are fused on BDT to give dithieno[2,3-*d*:2′,3′-*d*′]benzo[1,2-*b*:4,5-*b*′]dithiophene. Polymers with this repeat unit feature a more linear structure than their BDT counterparts,[68,69] which is beneficial for ordered interchain stacking. As a result, OPV devices with **32** and $PC_{71}BM$ delivered a PCE of 7.8% (*cf.* 5.0% for BDT counterpart **32a**). On the other hand, the strong aggregation of this highly fused polymer requires longer alkyl chains to maintain the solubility[69] and the synthesis of the monomer is more complex than BDT, increasing the cost of the material.

Polymer **33** explored the effect of BDT isomerism, using benzo[2,1-*b*:3,4-*b*′]dithiophene building block, with two thiophene rings facing the same direction.[70] Unlike common BDT with a 180° angle between connection sites, this BDT isomer features a 129° angle connectivity, resulting in a non-linear backbone and reducing the interchain stacking between polymer chains. This difference could be the reason for **33** presenting poorer photovoltaic performance (PCE 5.2%) than the BDT analog **34** (6.6%),[71] despite the higher V_{OC} of 0.82 V *vs.* 0.70 V in the former devices.

A light-element analog of BDT, benzodifuran (BDF), was used to build polymer **35**.[72] The smaller size of oxygen results in a more planar backbone and closer π–π stacking in **35** (3.57 Å) compared to BDT-bearing analog **D18** (3.65 Å, polymer **75** below). Recent comparative studies of ternary devices (with $PC_{71}BM$ and NFA **Y6-1O**, Fig. 6) showed a higher PCE (>17%) for **35** compared to **D18**, supporting the potential of the BDF building block in future development of OPV materials.

Terpolymers. Another strategy for fine-tuning the donor material is based on random copolymerization with a third comonomer. This third unit can be either a donor or an acceptor, and it can serve to extend the light absorption (usually in the short wavelength region), influence the energy levels and regulate the aggregation of polymer chains.[73] A thiophene unit was introduced into the BDT-pyridopyrazine polymer in **36**.[74] **36** presented a wider absorption spectrum between 350 and 600 nm compared to the parent copolymer, yielding higher

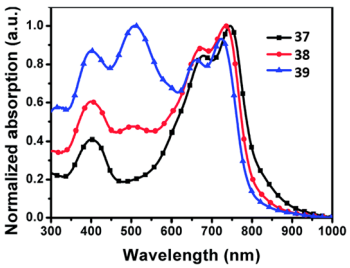

Fig. 7 Absorption spectra of terpolymers **37–39** as thin films. Copyright 2014 (RSC).[75]

photocurrent in solar cells. However, replacing some electron-withdrawing pyridopyrazine units with electron-donating thiophene slightly upshifted the HOMO level and slightly reduced V_{OC} in the **36**-based device by 0.03 V. **37–39** were synthesized with a varied ratio of DPP and thiophene–vinylene–dithienyl–benzothiadiazole units.[75] As the amount of BT-containing unit increases, a new absorption band appears at 450–580 nm owing to the side-chain chromophore (Fig. 7). As a result, **39** achieved a broad absorption over the entire solar spectrum and delivered higher short-circuit current density (J_{SC}) than **37** and **38**.

One of the drawbacks of the random copolymerization approach to terpolymers is the lack of control over the polymer sequences of the three moieties, which is unfavorable for the crystallinity of the polymer domains and may cause significant batch-to-batch variability. In principle, these problems can be mitigated by developing regioregular terpolymers, albeit at the cost of much higher synthetic complexity. This idea has been probed by Lee and coworkers who compared regioregular **40** with its regiorandom analog **41**. The former presents a redshifted absorption with a 0.17 eV smaller bandgap and 40 times higher hole mobility than the latter. As a result, a significantly improved PCE of 5.6% was obtained for **40** : $PC_{71}BM$ blends (*cf.* 1.1% for **41**).[76]

Side-chain engineering

Solubilizing chains. Modifying side chains on the BDT unit is another efficient strategy to tune the electronic and photovoltaic properties of BDT copolymers (Fig. 8 and Table 3). These side chains are incorporated into polymers to improve solubility

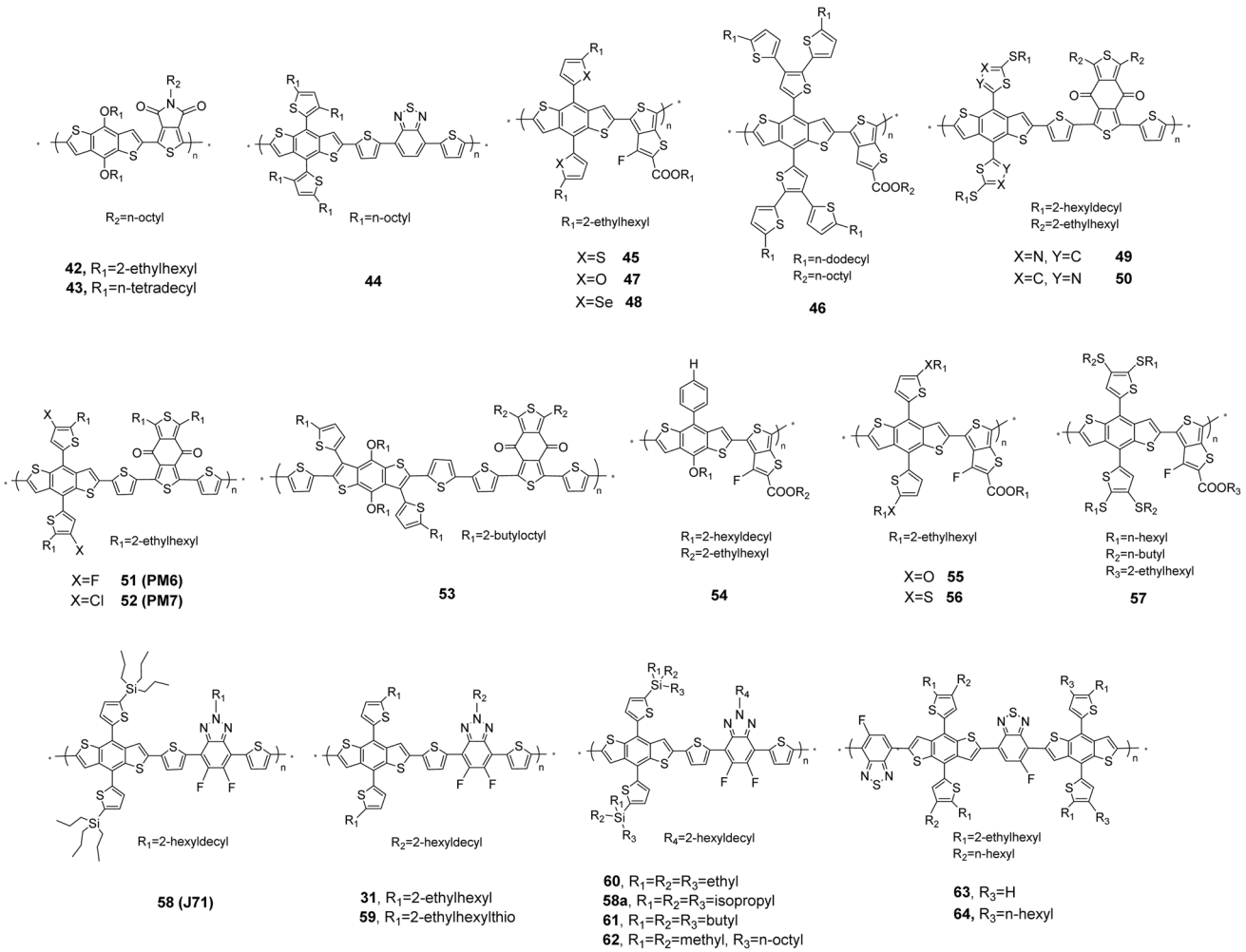

Fig. 8 Side chain engineering in D–A copolymers **42–64**.

Table 3 Optical, electronic, and photovoltaic performances of polymers **42–64** (Fig. 8)

	Polymer properties				OPV device						
	λ_{max}[a] (nm)	E_g[a] (eV)	HOMO[b] (eV)	LUMO[b] (eV)	wt/wt (acceptor)	V_{OC} (V)	J_{SC} (mA cm^{-2})	FF (%)	PCE (%)	Ref.	Year of report
42	627	1.73	−5.4	—	1 : 1.5 ($PC_{61}BM$)	0.85	12.5	65	7.3	80	2010
43	—	—	—	—	1 : 1.5 ($PC_{71}BM$)	0.93	8.3	53	3.8	80	2013
44	596	1.75	−5.31	−3.44	1 : 2 ($PC_{71}BM$)	0.92	10.7	57.5	5.7	84	2010
45	—	1.58	−5.22	−3.64	1 : 1.5 ($PC_{71}BM$)	0.8	15.7	74.3	9.4	85	2013
46	618	1.65	−5.64	−3.99	1 : 1.5 ($PC_{71}BM$)	0.9	4	46.6	1.7	86	2016
47	720	1.55	−5.19	−3.64	1 : 1.5 ($PC_{71}BM$)	0.69	11.8	64.8	5.3	85	2014
48	699	1.58	−5.29	−3.71	1 : 1.5 ($PC_{71}BM$)	0.81	16.6	65.6	8.8	85	2014
49	619	1.82	−5.43	−3.48	1 : 1.2 (BTP-eC9)	0.83	26.4	68.6	15.0	88	2024
50	636	1.77	−5.38	−3.53	1 : 1.2 (BTP-eC9)	0.83	19.5	39.4	6.4	88	2024
51	570	1.8	−5.45	−3.65	1 : 1.2 (Y6)	0.83	25.3	74.8	15.6	89	2019
52		—	−5.51	—	1 : 1 (IT-4F)	0.86	21.8	77	14.4	91	2018
53	592	1.90	−5.58	−3.54	1 : 1.4 (Y6)	0.82	26.6	72.5	15.8	92	2023
54	675	1.68	−5.10 (UPS)	−3.42	1 : 1.5 ($PC_{71}BM$)	0.80	17.4	67.5	9.4	31	2016
55	726	1.53	−5.18	−3.15	1 : 1.5 ($PC_{71}BM$)	0.73	15.2	64.4	7.1	93	2014
56	716	1.57	−5.41	−3.27	1 : 1.5 ($PC_{71}BM$)	0.84	15.3	65.5	8.4	93	2014
57	685	1.63	−5.5	—	1 : 1.5 ($PC_{71}BM$)	0.98	10.2	45	4.5	94	2016
58	587	1.96	−5.4	−3.24	1 : 1 (ITIC)	0.94	17.3	70.0	11.4	95	2016
31	538	1.96	−5.21	−2.99	1 : 1 (ITIC)	0.73	13.1	57.8	5.5	67	2016
59	598	1.93	−5.32	−3.08	1 : 1 (ITIC)	0.91	16.3	60.4	9.0	96	2016
60	580	1.99	−5.37	−2.91	1 : 1.5 (m-ITIC)	0.92	18.1	69.8	11.6	96	2018
58a	578	1.98	−5.42	−3.29	1 : 1.5 (m-ITIC)	0.96	16.4	65.0	10.2	96	2018
61	576	1.98	−5.46	−2.92	1 : 1.5 (m-ITIC)	0.97	16.5	66.9	10.7	96	2018
62	526	1.99	−5.56	−3.06	1 : 1.5 (m-ITIC)	0.99	15.9	61.2	9.6	96	2018
63	678	1.56	−5.15	−3.69	1 : 1.4 ($PC_{61}BM$)	0.90	14.2	61.1	7.4	97	2014
64	668	1.58	−5.20	−3.62	1 : 1.4 ($PC_{61}BM$)	0.90	10.8	60.8	5.7	97	2014

[a] In thin films, bandgap derived from absorption onset. [b] measured with cyclic voltammetry.

and regulate interchain aggregation. They are typically placed in the 4,8-positions of the BDT unit and, therefore, do not affect the planarity of the polymer backbone. Alkyl, alkylthio and alkoxy side chains have been used in BDT-based homopolymers since the early days[15,27,77,78] and are commonly exploited in corresponding copolymers. For example, a derivative of **15** with branched side chains was the first polymer showing a PCE over 7% in solar cells with $PC_{71}BM$.[79]

Fréchet and co-workers found that the size and shape of side chains on BDT can influence the polymer backbone orientation relative to the substrate by comparing **42** bearing branched 2-ethylhexyl chains to **43** with *n*-tetradecyl chains.[80] Grazing-incidence X-ray scattering (GIXS) data shows that the π-stacking ($q = 1.76$ Å^{-1}; *d*-spacing ~3.6 Å) is preferentially aligned in the out-of-plane direction in **42**, indicating the preferential "face-on" orientation, but is isotropically distributed in **43** (Fig. 9). Accordingly, **42** : $PC_{71}BM$ solar cells displayed an increased J_{SC} and fill factor (FF) leading to almost doubled PCE (7.3%) compared to **43** (3.8%).

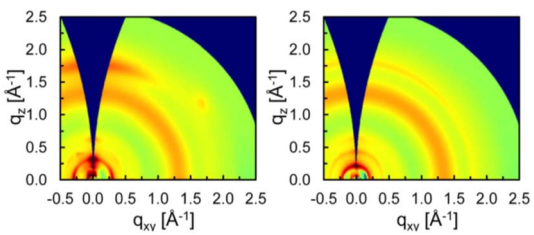

Fig. 9 GIXS patterns of (left) **42** and (right) **43** in optimized BHJs with $PC_{71}BM$. Copyright 2023 (RSC).[80]

Extending side chain conjugation. A very important feature of the BDT building block is the possibility to extend the conjugation in the second direction, orthogonal to the main backbone, through unsaturated substituents in 4,8-positions. Apart from changing the electronic levels and morphology of the polymer, such an extension also broadens the absorption band in the short-wavelength region leading to more efficient solar cells.[18,81] One of the simplest functional groups to extend the conjugation is the ethynyl group. Triispropylsilylethynyl and dialkoxyphenylethynyl groups have been used as side chains and the corresponding polymers achieved PCEs up to 6% with PCBM.[82,83]

A more versatile way to extend the side-chain conjugation in BDT polymers is based on aromatic and heteroaromatic substituents. The first D–A alternating copolymer with thienyl-substituted BDT **44** was reported in 2010. **44** has higher absorption in the short-wavelength region (400–500 nm) than its alkoxy counterpart **11** due to conjugated thiophene substituents. A PCE of ~5.7% was obtained in OPV devices with **44** : $PC_{71}BM$.[84] A higher PCE of 7.6% has been achieved with another thienyl-BDT copolymer **45**.[85] **45** has a redshifted absorption by 25 nm and a higher absorption coefficient than its analog **15**, which originates from the extended conjugation through alkylthienyl side chains and, possibly, a better π–π stacking.

The HOMO level of **45** was 0.08 eV lower than alkoxy-substituted **15**, contributing to a higher V_{OC} of 0.79 V and giving a PCE of 7.6% for the **45** : $PC_{71}BM$ cell. Installing two more thiophene groups on each thiophene substituent in **45** resulted in a further reduction of the HOMO level to −5.64 eV for **46** affording an enhanced V_{OC} of 0.90 V for the **46** : $PC_{71}BM$ device.[86] However, the J_{SC} of the corresponding device is only 4 mA cm^{-2}, much lower than that of its mono-thiophene analog **45**, which might be due to increased steric hindrance and less ordered intermolecular packing introduced by adjacent thiophene groups.

While thienyl and other aryl rings on BDT are useful for extending the conjugation and broadening the absorption,[85] this effect is limited by their twist with respect to the polymer backbone. Zhang *et al.* found that the smaller furyl substituents in **47** display a lower twist with respect to BDT (calculated dihedral angle of 34°) compared to thienyl (59°) and selenophenyl (61°) groups in the analogous polymers **45** and **48**.[87] As a result, **47** presents a stronger absorption in the short-wavelength region (at ∼500 nm) than **45** and **48**, due to improved side chain conjugation. Perhaps more importantly, **47** packs in the solid state with a closer π–π stacking distance of 3.63 Å, compared to **45** and **48** (3.94 Å), which in principle should be beneficial for the hole transport. However, unfortunately, a relatively low PCE of 5.3% was achieved in the **47** : $PC_{71}BM$ BHJ (*cf.* ∼9% for **45** and **48**) which was attributed to the excessive crystallization/phase separation in this highly planar polymer.

Introducing heteroatoms into aryl substituents can lead to a less twisted BDT structure. 1,3-Thiazole connected to BDT at its 5-position inherits the conformation of thiophene, with a dihedral angle of 59° in **49**.[88] Altering the connecting point to the 2-position results in a significantly smaller dihedral angle of 24° in **50**, due to reduced steric repulsion. However, the more planar structure of **50** causes excessive intermolecular interactions and unfavorable phase separation in a blend with NFA **BTP-eC9**, resulting in a much lower PCE of 6.4% compared to 15.0% for **49**.

Halogenation is one of the common strategies employed to lower the energy levels of conjugated polymers. It was explored in BDT polymer **51** by using ring-fluorinated alkylthiophene substituents and resulted in one of the most popular BDT semiconductors, widely known as **PM6**.[89] **51** exhibits a HOMO level deeper by 0.22 eV than its non-fluorinated analog **14**, similar to that of **26** with a fluorinated thiophene linker on the backbone. Moving fluorine from the 4-position to 3-position on the thienyl substituent generates additional steric clashes

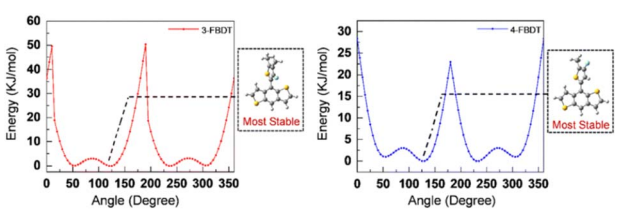

Fig. 10 Torsional energy profiles of thienyl-BDT with F on different positions of the thienyl side chain. Copyright 2023 (RSC).[86]

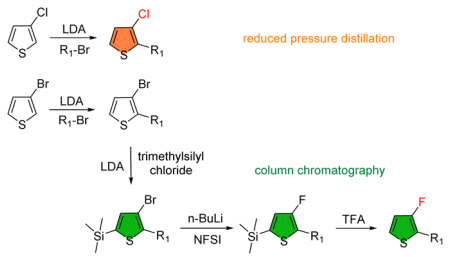

Scheme 2 Synthesis route of thienyl side chains for **51** and **52**.

between F and β-H on BDT and increases the torsion energy barriers from 5.5 to 12 kcal mol^{-1} although the minimum energy conformation is not significantly changed (Fig. 10).[90] The restricted rotation of the side chains breaks the symmetry of the polymer chains, resulting in improved solubility and processability in a non-halogenated solvent, THF.

52 (also known as **PM7**) is an analog of **51** where the F atoms are replaced with Cl.[91] The chlorinated thiophene building block requires fewer synthetic steps and is easier to purify than the fluorinated thiophene (Scheme 2), lowering the cost of the polymer. Also, **52** exhibits a HOMO of −5.40 eV, lower than −5.33 eV for **51** due to lower π-donation from Cl, but its absorption spectrum, film morphology and hole mobility, are very similar to those of **51**.

53 was designed with four side chains on the BDT unit: two alkylthienyl groups attached to 3,7-positions and two alkoxy groups attached to the 4,8-positions.[92] It exhibits a λ_{max} of 550 nm in solution, which is blue-shifted compared to that of **14** (581 nm). Such behavior suggests a less efficient conjugation in **53**, which can be reasonably attributed to the large dihedral twist of the backbone with such an overcrowded building block.

Most BDT building blocks used in D–A copolymers are substituted symmetrically. Breaking this symmetry was explored in 2016 by the Yang group who made a series of D–A copolymers of BDT bearing one alkoxy and one aryl group, including polymer **54**.[31] Devices of **54** with $PC_{71}BM$ showed a 0.06 V increase of V_{OC} compared to the symmetric dialkoxy-substituted **15** and also a ∼4 mA cm^{-2} increase of J_{SC} compared to the symmetric diaryl-substituted polymer, which was attributed to better chain stacking.

Varying the type and number of substituents on the pendant aryl rings on BDT is a widely used strategy to fine-tune the electronic properties of polymers. **55** and **56** have the same backbone structure with alkoxy and alkylthio chains on the thiophene substituents, respectively.[93] Due to the stronger electron-donating effect of the alkoxy group, **55** displays a higher HOMO of −5.18 eV than its alkylthio counterpart **56** (−5.41 eV). Accordingly, the V_{OC} of corresponding devices increases from 0.74 V for **55** to 0.84 eV for **56** to as high as 0.98 V for **57** with two alkylthio chains on each thiophene substituent (Table 3).[94]

The trialkylsilyl group on thienyl substituents can effectively decrease the HOMO level of polymers due to the electron-withdrawing effect of the silyl group through σ*(Si)–π(C) hyperconjugation. As a result, **58** (also known as **J71**) bearing

a bulky trialkylsilyl group presents a deeper HOMO of −5.4 eV, compared to alkylated **31** (−5.21 eV) and alkylthiolated **59** (−5.32 eV).[67,95] The modulation of alkyl chains on the trialkylsilyl group was used in fine-tuning the solid state properties of polymers (**58**, **58a-62**).[96] The polymers with shorter and linear alkyl chains on the silicone atom displayed closer π–π stacking, higher absorption coefficient and higher J_{SC} and FF values. Of all 5 polymers, devices of **58** with **m-ITIC** achieved the highest PCE of 12.1%.

Varying the number and the length of alkyl chains on thienyl substituents can be used to fine-tune the interchain stacking of BDT polymers. The importance of such tuning has been demonstrated by Watkins, Muellen and co-workers in polymer **63**, which combines both monoalkylthienyl-BDT and dialkylthienyl-BDT units. This polymer packs significantly closer and has a better crystallinity than its analog **64** with all dialkylthienyl-BDT.[97] As a result, **63** has higher hole mobility (1.5×10^{-3} cm^2 V^{-1} s^{-1}) and shows a significantly increased PCE of 7.2% compared to 5.7% for **64** (in BHJs with $PC_{61}BM$).

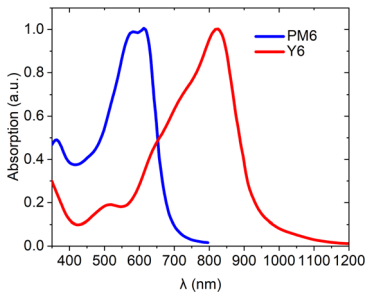

Fig. 11 Complementary absorption of NFA **Y6** and **PM6** films showing a complementarity of absorption of wide band-gap polymers with NFAs.

Optimizing BDT polymer donors for OPV application with non-fullerene acceptors

The rise of low-band-gap NFAs (Fig. 6) in the field of OPV has created a need for polymer donors with new properties, optimized for these acceptors to achieve high PCEs. Currently, the most efficient NFAs have strong absorption in the red-infrared region of the spectrum and are nearly transparent in the blue-green region. Accordingly, they require polymer donors with a wider bandgap and a complementary absorption profile to maximize the harvesting of solar radiation (Fig. 11). Furthermore, there is an increasing demand for polymers that are processable in green solvents and are cost-effective. These properties can be achieved through the abovementioned main-chain engineering and side-chain engineering strategies. In this section, we will summarize the effort on the design of wide bandgap BDT polymers and discuss the key examples of their application in high-performance OPV in conjunction with low band-gap NFAs.

BDT copolymers with benzodithiophenedione

One of the most successful series of BDT polymers is based on its copolymerization with the BDD acceptor, among which **14** (**PBDB-T**, Fig. 12) is the first example that delivered promising PCE and is still widely used today. The BDD unit is easy to synthesize *via* Friedel–Crafts acylation, allows the solubility of the polymer to be tuned through additional alkyl chains on the outer thiophene ring, and planarizes the connection with thiophene linkers *via* non-covalent C═O···S interactions. In 2016, a device with a **14**:**ITIC** active layer yielded a PCE of 11.2%, for the first time outperforming the control device

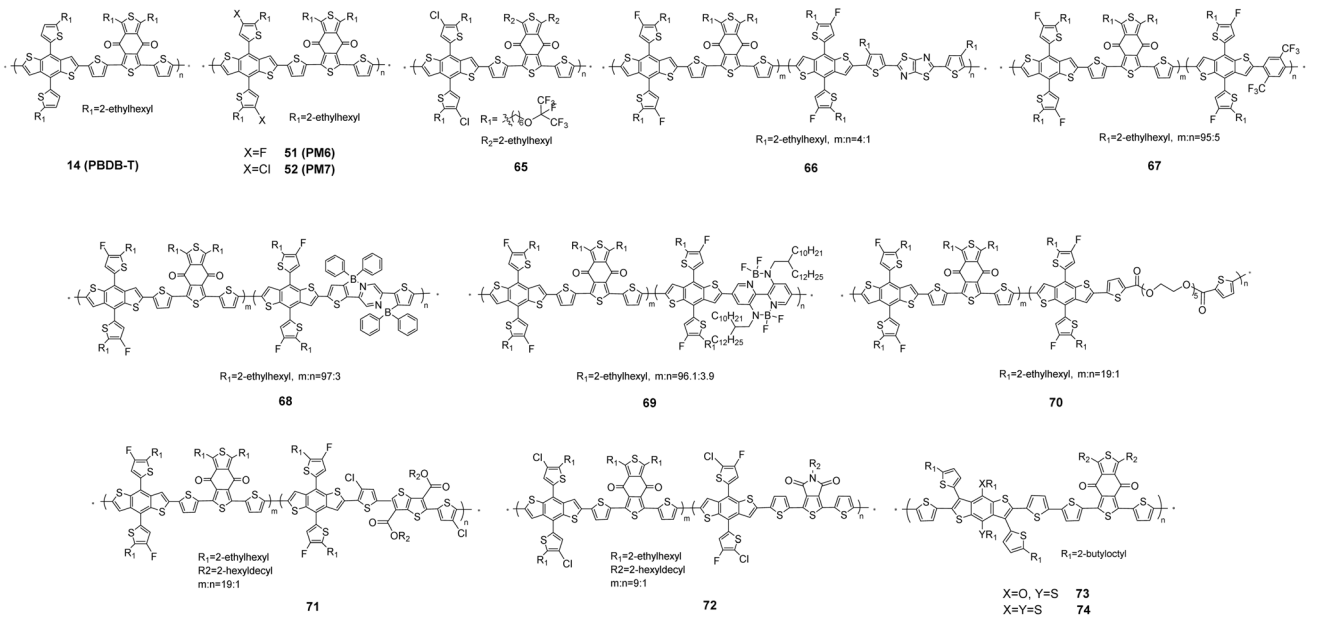

Fig. 12 Representative PBDB-T type polymers with benzodithiophenedione acceptors used in high-performance OPVs (see Table 4 for their properties).

Table 4 Optical, electronic, and photovoltaic performance of PBDB-T type polymers (Fig. 12)

	Polymer properties				OPV device						
	λ_{max} (nm)	E_g (eV)	HOMO (eV)	LUMO (eV)	wt/wt (acceptor)	V_{OC} (V)	J_{SC} (mA cm^{-2})	FF (%)	PCE (%)	Ref.[a]	Year of report[a]
14	622	2.05 (E_g^{EC})	−5.23	−3.18	1 : 1 (ITIC)	0.90	16.8	74.2	11.2	98	2016
					1 : 1 : 0.1 (Y14 : SM6)	0.84	27.5	73.6	17.1	104	2022
51	570	1.8	−5.45	−3.65	1 : 1.2 (Y6)	0.83	25.3	74.8	15.6	106	2019
					1 : 1.2 (A4T-16)	0.88	21.8	79.8	15.2	107	2021
					0.8 : 0.2 : 1.2 (51 : 75 : L8-BO)	0.90	26.7	81.9	19.6	108	2022
52		—	−5.51	—	1 : 1 (IT-4F)	0.86	21.8	77	14.4	91	2018
65	—	1.84	−5.55	−3.7	1 : 1.2 (L8-BO)	0.90	26.1	79.3	18.7	124	2024
66	—	1.86	−5.52	−3.59	1 : 1 : 0.2 (L8-BO : BTP-2F2Cl)	0.88	27.2	80.1	19.2	129	2022
67	615	1.83	−5.52	−3.38	1 : 1.2 (L6-BO)	0.84	28.0	77.2	18.2	131	2023
68	—	1.67	−5.46	−3.46	1 : 1.2 (L8-BO)	0.91	26.6	78.9	19.0	132	2023
69	570	—	−5.48	−3.45	1 : 1.2 (L8-BO)	0.91	26.7	79	19.1	133	2023
70	617	1.82	−5.55	−3.73	1 : 1.2 (BTP-eC9)	0.84	27.1	78.0	17.7	134	2022
71	619	1.84	−5.56	−3.72	(BTP-eC9)	0.86	26.8	80.0	18.4	135	2023
72	—	1.76	−5.63	−3.66	1 : 1.2 (L8-BO)	0.91	25.6	78.1	18.3	136	2024
73	560	1.85	−5.64	−3.62	1 : 1.3 (Y6)	0.82	26.9	68.2	15.0	137	2024
74	564	1.84	−5.61	−3.57	1 : 1.3 (Y6)	0.80	27.3	61.1	13.4	137	2024

[a] Refer to the publication of the corresponding OPV device.

Table 5 Optical, electronic, and photovoltaic performance of D18-type polymers (Fig. 13)

	Polymer properties				OPV device						
	λ_{max} (nm)	E_g (eV)	HOMO (eV)	LUMO (eV)	wt/wt (acceptor)	V_{OC} (V)	J_{SC} (mA cm^{-2})	FF (%)	PCE (%)	Ref.[a]	Year of report[a]
75	581	1.98	−5.44	−3.47	1 : 1.6 (Y6)	0.86	27.7	76.6	18.2	140	2020
					1 : 1.2 (L8-BO)	0.91	26.5	80.7	19.7	141	2023
76	576	2.00	−5.49	−3.49	1 : 1.4 : 0.2 (Y6 : $PC_{71}BM$)	0.87	26.8	77.0	18.0	147	2021
					(BTP-4F-P2EH)	0.92	27.9	80.8	20.8	148	2024
77	576	1.97	−5.52	−3.64	1 : 1.2 (L8-BO)	0.92	25.5	80.5	18.8	149	2024
78	545	1.91	−5.55	−3.42	1 : 1 (BTP-eC9-4F)	0.88	27.1	76.4	18.1	128	2022
79	569	1.82	−5.51	−3.35	1 : 1.2 (L8-BO)	0.90	25.9	77.4	18.1	150	2023
80	583	1.98	−5.31	−2.77	bilayer (Y6)	0.87	27.8	78.9	19.1	151	2024
81	581	1.98	−5.58	−3.68	1 : 1.2 (Y6)	0.87	27.0	78.7	18.4	152	2022

[a] Refer to the publication of the corresponding OPV device.

fabricated with the fullerene acceptor $PC_{71}BM$ (Table 4).[98] Since then, **14** has been used in a BHJ with a number of different NFAs.[99–103] In 2022, a ternary device with **14** and two NFAs (**Y14** and **SM16**) delivered a PCE of 17.1%, which remains the highest OPV performance of **14** to date.[104] In addition to high PCE, **14** can be processed in non-halogenated solvents and showed high stability in OPV devices.[105]

A great many analogs of **PBDB-T** (**14**) have been developed through the years. Hou *et al.* introduced the fluorine atom to the alkylthienyl side chains of BDT, making polymer **51**, which has become widely known as **PM6**.[89] **51** exhibits a deeper HOMO level of 0.22 eV than its non-fluorinated analog **14**. In 2019, OPV devices of **51** and **Y6** achieved an impressive PCE of 15.6% with V_{OC} of 0.83 V and FF of 74.8%, marking the emergence of the **Y6** series as the current state-of-the-art NFAs.[106] Later, a similarly high PCE of 15.2% was demonstrated with **51** and a synthetically simpler non-fused NFA **A4T-16**.[107] In a ternary system with **51**, **75** and **L8-BO**, the authors observed the formation of a multi-length scaled double-fibril network which they believe is responsible for the very high device efficiency of 19.6%.[108] Recently, a record efficiency of 19.7% was reported for **51**-based solar cells.[109] **51** has now become the benchmark polymer donor, widely used to test new NFAs,[99,110–113] unravel photophysical processes in OPVs[114,115] and explore new device engineering approaches, *e.g.* transparent,[116] stretchable,[117,118] and bilayer (quasi planar heterojunctions)[119] devices, interfacial engineering,[120] *etc.*

52 (**PM7**) is an analog of **51** where the fluorine atoms are replaced with Cl which has a lower HOMO and is synthetically simpler. OPVs with **52** have reached PCE between 14% and 17%

for several systems.[91,121–123] By incorporating a perfluoroisopropoxyalkyl group as the side chain on the **PM7** backbone an enhanced PCE of 18.7% was achieved for polymer **65** with NFA **L8-BO**.[124] The fluoroalkyl chains provide a handle to control the phase separation in the BHJ and a further increase of PCE to 19.1% was realized after fluorous solvent vapor annealing of the active layer.

Many high-efficiency donor polymers have been developed by incorporating a third comonomer and optimizing its ratio in the structure of **PM6 51** and **PM7 52**.[125–128] Random terpolymer **66** introduced a moderately electron-withdrawing thiazolothiazole (TTz) with thiophene linkers into **51**'s backbone.[129] The TTz-thiophene connection is almost planar while the BDD-thiophene link has a dihedral angle of 16°, which may explain the improved crystallinity and charge mobility of **66** compared to **51**. **66** exhibits excellent batch-to-batch reproducibility, and PCEs of *ca.* 18% were reported in blends of **66** with various NFAs (**Y6**, **BTP2F2Cl** and **L8-BO**).[129,130] The efficiency was further enhanced to 19.2% in a ternary blend of **66 : L8-BO : BTP2F2Cl**.

A simple 1,4-bis(trifluoromethane)benzene as a third comonomer in PM6 analog **67** significantly improves the solubility of the polymer, allowing the **67 : Y6-BO** active layer to be processed from a non-halogenated solvent (xylene), achieving a high PCE of 18.2%.[131]

Replacing 3% of the BDD unit in **PM6** with the zwitterionic borylated dithienopyrazine acceptor in polymer **68** (ref. 132) lowered the HOMO of the polymer allowing it to achieve a high V_{OC} of 0.91 V and a PCE of 19.0% for the **68 : L8-BO** device. An analogous terpolymer **69** with a structurally related BF_2-fused bipyridine acceptor was reported later.[133] The out-of-plane dipoles of the BF_2 group contribute to the strong interchain interactions and increase the crystallinity of **L8-BO** in the blend film and OPV devices with the **69 : L8-BO** active layer delivered a high PCE of 19.1%.

A non-conjugated terpolymer **70** was synthesized by incorporating a flexible penta(ethylene glycol) spacer in the **PM6** structure, as a means to enhance the mechanical properties of the film.[134] A stretchable device fabricated with **BTP-eC9** NFA yielded a PCE of 12.1%, with 80% of the efficiency retained at 22% strain. Meanwhile, regular devices with the same active layer fabricated from **70** in a non-halogenated solvent (toluene) delivered a high PCE of 17.7%.

Other examples of introducing third units in the **PM6**/**PM7** backbone include substituted thienothiophenes in **71** and thienopyrroledione in **72**.[135,136] **71** achieved a PCE of 18.4% and an outstanding FF of 80% with **BTP-eC9**. Binary devices with **72** and **L8-BO** yielded a PCE of 18.3% and an even higher PCE of 19.4% was achieved in ternary devices.

Polymer **73** was developed by breaking the symmetry of BDT.[137] This polymer with one alkylthio and one alkoxy side chain exhibits a reduced π–π stacking distance compared to its symmetric counterparts (**74** and **53**), which contributes to an increased hole mobility of 10^{-3} cm^2 V^{-1} s^{-1} in its blend with **Y6**. The BHJ devices **73 : Y6** yielded a PCE of 15.0%, higher than the 13.4% for **74** and 14.7% for **53**.

BDT copolymers with dithienobenzothiadiazole

Benzo[*c*][1,2,5]thiadiazole (BT) has been widely used in conjugated polymers and PCEs of up to 12% have been achieved with BDT-BT polymers and ITIC-type NFAs.[138] However, the high electron deficiency of BT typically leads to low bandgaps (<1.80 eV) in these polymers, which is not ideal for devices with the NIR-absorbing NFAs as it results in underutilization of the short-wavelength range of the solar spectrum.[139] One method to mitigate the strong electron-accepting ability of BT acceptor is by fusing it with electron-donating thiophenes to give dithienobenzothiadiazole (DTBT). In 2020, polymer **75** (also known as **D18**, Fig. 13) with BDT and DTBT moieties separated by thiophene linkers was reported.[140] **75** has a wide bandgap of 1.98 eV and a high hole mobility of 1.6×10^{-3} cm^2 V^{-1} s^{-1}. The BHJ device of **75** with **Y6** yielded a PCE of 18.2%. To mitigate the low solubility of **75**, a high-pressure coating method was developed. This method allowed high molecular weight **75** (85 kDa) to be processed at 100 °C and the fabricated devices with **L8-BO**

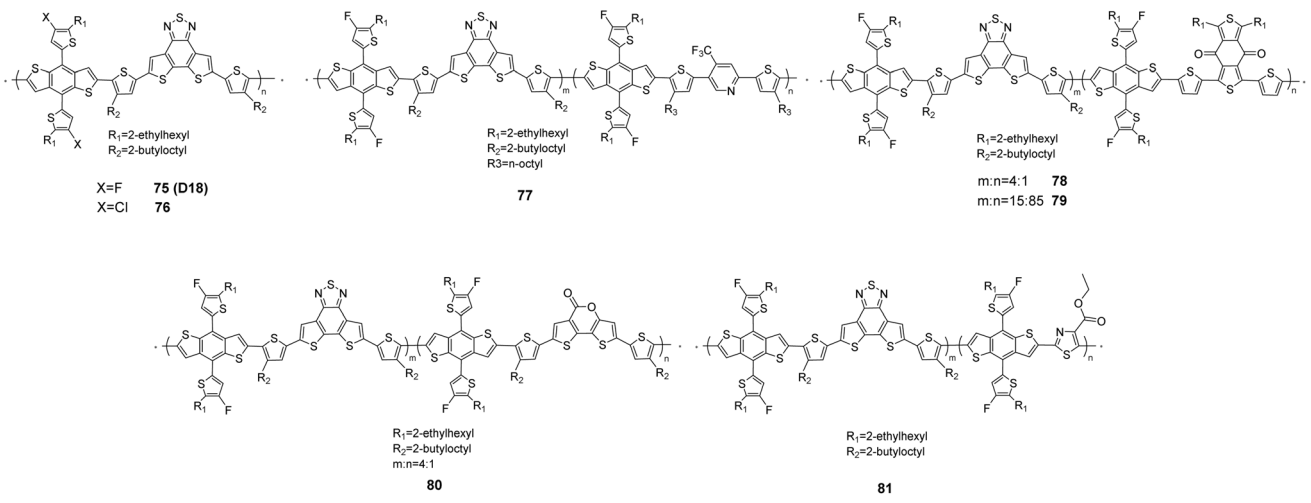

Fig. 13 Representative D18-type polymers with dithienobenzothiadiazole for high-performance OPVs (see Table 5 for their properties).

showed a very high PCE of 19.7%.[141] Other than traditional BHJ architecture, **75** was also utilized in a bilayer p-i-n quasi-planar heterojunction structure with a partial donor/acceptor intermixed phase delivering high PCEs around 19%.[141,142]

Many modifications of **75** (**D18**) have been explored to optimize the PCE of NFA-based OPVs.[143–146] The chlorination of thienyl substituents in **76** lowers the HOMO level to −5.49 eV (*cf.* −5.44 eV for **75**) and a PCE of 18.0% was achieved in the initial studies in the ternary **76 : Y6 :** $PC_{71}BM$ blend.[147] Furthermore, a record-breaking PCE of 20.8% was reported for **76**-based bilayer devices with **BTP-4F-P2EH** acceptor last year.[148]

The terpolymer strategy has been widely explored for **75**. Random terpolymer **77** with a *p*-trifluoromethylpyridine acceptor presented reduced aggregation tendency compared to **75** and delivered PCEs of >18% in a BHJ with various NFAs.[149] Both BDD and DTBT acceptor units were used in polymer **78**, which is effectively a mixed copolymer of **PM6** (**51**) and **D18** (**75**).[128] The new polymer displayed a much-enhanced solubility and temperature-dependent aggregation behavior in xylene, which is not observed for either of the corresponding parent copolymers. The optimized **78 : BTP-eC9-4F** device reached a PCE of 18.1%. Increasing the BDD : DTBT ratio from 1 : 4 in **78** to over 5 : 1 in **79** resulted in a bandgap reduction by 0.09 eV and a slightly increased HOMO.[150] Devices with **79 : L8-BO** showed high PCEs over 17.5% over the wide range of molecular weights, providing a much better reproducibility of device performance compared to the parent **PM6** and **D18** polymers.

A series of **D18**-type terpolymers was developed with a lactone-fused dithiophene unit.[151] Increasing the amount of lactone in the polymer backbone gradually changes the polymer film microstructure to edge-on orientation improving the miscibility with the acceptor (**Y6**). This optimization approach in polymer **80** allowed a PCE of 19.1% to be achieved in bilayer devices.

Another notable example of **D18**-type terpolymer was developed using an ester-substituted thiazole comonomer.[152] With only 5% thiazole *vs.* DTBT unit, **81** shows a decreased HOMO level (by 0.07 eV) and improved morphology, resulting in a PCE of 18.4% for **81 : Y6** devices.

BDT copolymers with benzotriazole

Compared to the widely used benzothiadiazole, benzotriazole (BTz), with its electron-donating nitrogen, acts as a weaker acceptor, leading to wider bandgap polymers. The extra alkyl chain on the nitrogen atom allows for further fine-tuning of the solubility and packing of BTz-containing polymers. To obtain HOMO levels that pair better with NFAs, fluorine atoms are typically placed on 5,6-positions of alkylated BTz units.

The first BDT copolymer with difluoro-BTz was reported in 2012 (ref. 153) and later used in combination with NFAs.[154,155] A number of thienyl-BDT/difluoro-BTz copolymers with various substituents (*e.g.* alkyl, alkylthio and alkylsilyl groups) have been developed (Fig. 14 and Table 6).[67,95,96] Due to the electron-withdrawing effect of the alkylthio substituents, **59** and **82** display a redshifted absorption (by *ca.* 10 nm) and decreased HOMO by 0.1 eV compared to its alkyl counterpart **31**.[67] This HOMO stabilization leads to higher V_{OC} of 0.91 V for **59** and 0.89 V for **82** respectively, compared to 0.73 V for **31** (BHJs with **ITIC**).

Bulky trialkylsilylthienyl substituents are used in a popular BDT-BTz copolymer **58** (also known as **J71**).[95] Apart from improving the solubility of **58**, trialkylsilyl groups deepen the HOMO of the polymer compared to its alkyl counterpart **31**. The first solar cell based on **58** yielded a PCE of 11.4% and a V_{OC} of 0.94 V with **ITIC**,[95] and further device optimization delivered PCEs of up to 16.5%.[156–159]

Between 2019 and 2022, more than ten BDT-BTz polymers were reported with PCEs >14%.[160–165] In 2023, a record (for BDT-BTz polymers) PCE of 17.1% was reported with polymer **83** and **Y18** acceptor.[69] This polymer presented a high carrier mobility of $\sim 10^{-3}$ cm^2 V^{-1} s^{-1} and a high J_{SC} of 26.8 mA cm^{-2}, which is the highest value for all BDT-BTz polymers. Notably, **83** is processable in non-halogenated solvents (xylene), with a respectable PCE of 16.9% for **83 : Y18** devices.

The electron-accepting ability of difluoro-BTz can be increased by replacing fluorine with other substituents. **84** with chlorine-bearing BTz presents a slightly lower (by 0.03 V) HOMO and almost identical bandgap to **57**.[166] It should be noted, however, that the substitution of F with Cl results in a less planar and less rigid polymer backbone (Fig. 15). The BHJ with **84** and NFA **ZITI** delivered a PCE of 14.4%.

Electron-withdrawing cyano groups significantly decrease the energy level and **85** exhibits a HOMO of −5.50 eV, 0.29 eV lower than the fluorine analog **31**.[167] As a result, the **85 : Y6** blend yielded a V_{OC} of 0.86 V (0.74 V for **31 : Y6**) and a PCE of 15.2%. Dicarboxyimide substitution on BTz also results in a lowered HOMO (0.13 eV) and a smaller bandgap (0.15 eV) than **58**.[168] This strategy was used to develop polymer **86**, which has a HOMO of −5.45 eV and delivers a V_{OC} of 0.81 V and a PCE of 16% in the BHJ with **Y6**.[169] The same acceptor was later used in polymer **27** affording a PCE of 16.8% with **Y6**.[64]

On the other hand, fusing thiophene on both sides of the BTz unit makes it less electron-deficient than difluoro-BTz and results in a wider bandgap (2.01 eV) for **87** (1.94 eV for difluoro-BTz analog **83**).[170] Removal of fluorine atoms from the BTz unit eliminates the S···F interactions between the acceptor and adjacent π-linkers, resulting in a twisted backbone with a 13° dihedral angle which weakens both intramolecular and intermolecular electronic coupling. The lower absorption of the solar radiation results in the low J_{SC} of 21.2 mA cm^{-2} of **87 : Y18** devices (*cf.* 26.8 mA cm^{-2} for **83 : Y18** devices). Several other polycyclic BTz acceptors have been explored and a PCE of 15.5% has been reported for **88**.[171] While the synthetic complexity of these linker/acceptor units will limit its application, this example is notable in using a diphenyl-BDT (rather than dithienyl-BDT) polymer in high-performance OPVs.

BDT copolymers with quinoxaline

The two nitrogen atoms provide quinoxaline (Qx) a moderate electron-withdrawing character for developing wide bandgap copolymers. Multiple positions on the unit allow for installing side chains to fine-tune the optoelectronic properties and

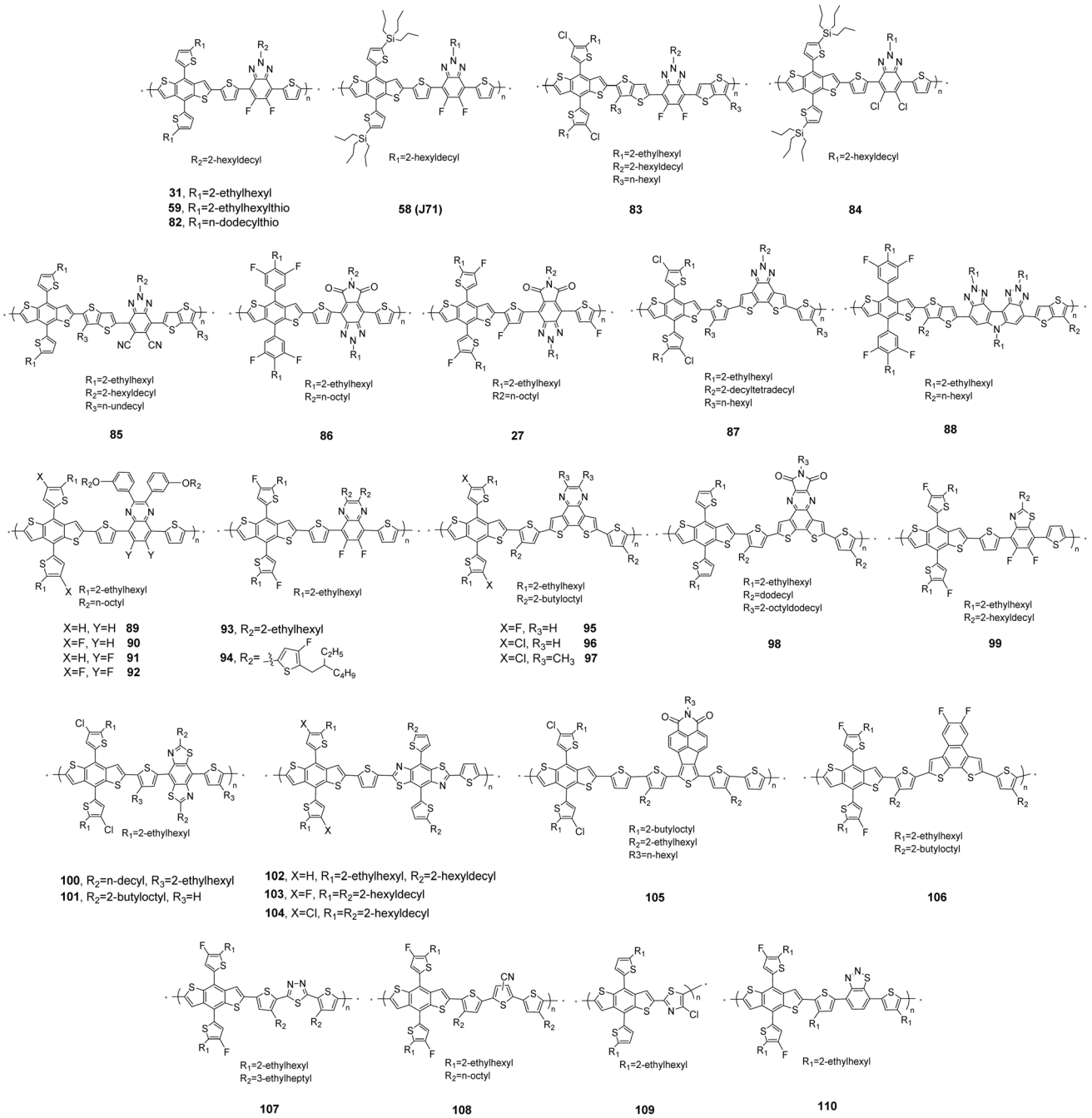

Fig. 14 Representative polymers with BTz, Qx and other acceptors used in OPVs with NFAs (see Table 6 for their properties).

aggregation of corresponding materials. Several BDT copolymers with Qx and its derivatives have shown high OPV performance (PCE 11–19%) in combination with NFAs (Fig. 14 and Table 6).[172–176] The impact of the number and position of fluorine substituents on the optical properties and energy levels was studied in Qx-based polymers **89–92**.[177] The absorption coefficient of the polymer is increased when more fluorine atoms are incorporated. HOMO levels of all three fluorine-bearing polymers (**90–92**) are lower than that of the non-fluorinated **89**. When these polymers were paired with **ITIC**, a V_{OC} of up to 0.95 V and a PCE of up to 11.3% was achieved in **92**-based devices.[172]

Y. Li and co-workers studied the role of side chains on the Qx unit in polymers **93** and **94**.[174] As expected, **94** with the conjugated fluorothienyl substituents on Qx presented a significantly lower bandgap and a 70 nm redshifted absorption compared to **93** with simple alkyl substituents. Furthermore, a reduced π–π stacking distance in **94** results in twice higher hole mobility to **93** and a higher PCE of 17.6% in **94 : Y6** devices.

A fused dithienoquinoxaline unit was incorporated in **95**.[175] Fusion with electron-rich thiophene decreases the electron deficiency of Qx and, as a result, **95** presents a wider bandgap of 2.07 eV, which improves the absorption of the higher energy

Table 6 Optical, electronic, and photovoltaic performances of polymers with BTz, Qx and other acceptors (Fig. 14)

	Polymer properties				OPV device						
	λ_{max} (nm)	E_g (eV)	HOMO (eV)	LUMO (eV)	wt/wt (acceptor)	V_{OC} (V)	J_{SC} (mA cm^{-2})	FF (%)	PCE (%)	Ref.[a]	Year of report[a]
31	538	1.96	−5.21	−2.99	1 : 1 (ITIC)	0.73	13.1	57.8	5.5	67	2016
59	550	1.93	−5.32	−3.08	1 : 1 (ITIC)	0.91	16.3	60.4	9.0	96	2016
82	552	1.93	−5.32	−3.08	1 : 1 (ITIC)	0.89	17.4	61.5	9.5	96	2016
58	587	1.96	−5.4	−3.24	1 : 1 (ITIC)	0.94	17.3	70.0	11.4	95	2016
83	595	1.93	−5.48	−3.55	1 : 1.2 (Y18)	0.85	26.8	74.9	17.1	69	2023
84	544	1.97	−5.30	−3.50	1 : 1 (ZITI)	0.94	21.3	72.5	14.4	166	2019
85	647	1.74	−5.50	−3.67	1 : 1.1 (Y6)	0.86	25.4	69.5	15.2	167	2022
86	—	1.87	−5.45	−3.14	1 : 1.2 (Y6)	0.81	26.5	72.6	15.7	169	2019
27	642	1.72	−5.55	−3.83	1 : 1 (Y6)	0.85	26.3	75.5	16.8	64	2020
87	529	2.01	−5.49	−3.48	1 : 1.2 (Y18)	0.86	21.2	68.2	12.5	170	2023
88	573	1.97	−5.34	−3.63	1 : 1.2 (eC9-2F)	0.81	25.3	75.7	15.5	171	2024
89	636	1.64	−5.05	—	1 : 1 (ITIC)	0.69	16.2	59.9	6.7	177	2017
90	619	1.66	−5.19	—	—	—	—	—	—	177	2017
91	600	1.68	−5.19	—	1 : 1 (ITIC)	0.83	17.2	62.5	8.9	177	2017
92	583	1.73	−5.35	—	1 : 1 (ITIC)	0.95	17.9	66.8	11.3	177	2017
93	565	1.88	−5.55	−2.91	1 : 1.3 (Y6)	0.84	26.0	70.8	15.6	174	2021
94	634	1.71	−5.64	−3.18	1 : 1.3 (Y6)	0.85	26.6	77.9	17.6	174	2021
95	—	2.07	−5.41	−2.82	1 : 1 : 0.2 (eC9-2Cl : F-BTA3)	0.88	26.7	80.9	19.0	175	2021
					1 : 1.2 (TBT-13)	0.79	25.9	77.9	16.1	179	
96	—	2.05	−5.39	−2.86	1 : 1 : 0.2 (BTP-eC9 : BTA3)	0.84	26.9	79.6	18.0	176	2021
97	—	2.00	−5.26	−2.76	1 : 1.2 (PY-IT)	0.92	24.3	80.7	18.0	181	2022
98	530	1.80	−5.47	−3.72	1 : 1.4 (PY-IT)	0.90	26.5	78.6	18.8	182	2024
99	518	2.06	−5.43	−3.37	1 : 1.2 (L8-BO)	0.90	26.7	77.6	18.6	186	2023
100	531	2.02	−5.66	−3.47	1 : 1.8 (Y6)	0.81	24.7	75.4	15.1	187	2021
101	540	2.00	−5.54	−3.65	1 : 1.2 (PY-IT)	0.95	24.6	73.7	17.2	188	2023
102	—	—	−5.45	−3.47	0.8 : 0.2 : 1.2 (51 : 102 : PY-IT)	0.94	24.7	76.3	17.6	189	2023
103	—	—	−5.55	−3.57	1 : 0.15 : 1.2 (51 : 103 : BTP-eC9)	0.85	28.2	78.3	18.7	190	2024
104	—	—	−5.59	−3.64	1 : 0.15 : 1.2 (51 : 104 : BTP-eC9)	0.85	27.5	78.2	19.0	190	2024
105	557	1.98	−5.47	−3.49	1 : 1.5 (N3)	0.86	26.6	77.3	17.6	191	2021
106	562	2.05	−5.39	−3.49	1 : 1.2 (BTP-eC9-4F)	0.91	26.8	67.1	16.2	192	2024
107	—	2.12	−5.64	−3.52	1 : 1 (IT4F)	0.96	20.5	74	14.5	193	2021
108	552	1.92	−5.58	−3.66	1 : 1.35 (Y6)	0.85	27.2	74.3	17.1	194	2021
109	537	2.00	−5.63	−3.54	(BTP-eC9-4F)	0.86	26.1	66.1	15.0	195	2024
110	556	1.93	−5.53	−3.17	1 : 1.2 (Y6)	0.87	28.2	77.3	19.0	196	2024

[a] Refer to the publication of the corresponding OPV device.

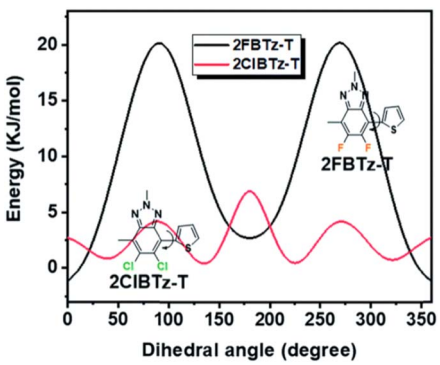

Fig. 15 The twisting barriers of chlorine/fluorine substituted BTz with an adjacent thiophene linker calculated by the DFT method. Copyright 2019 (RSC).[166]

photons. The device of **95** with **eC9-2Cl** delivered a PCE of 17.7%, and the device performance can be further enhanced to 19% by introducing a third component, **F-BTA3**, or other additives.[178] In a recent report, a PCE of 16.1% was delivered by the BHJ of **95** and fully non-fused NFA **TBT-13**.[179] The chlorinated polymer **96** has similar optical bandgap and energy levels as its fluorinated analog **95**, and similarly high-performing ternary devices with PCEs of 18.0%[176] and even 19.0%[180] have been reported for this polymer. The processability of **96** in green (non-chlorinated) solvents can be improved by methylating the pyrazine ring. Indeed, the so-designed polymer **97** can be processed from toluene and showed a remarkable PCE of 18.0% in a binary device with a polymer acceptor, **PY-IT** (Fig. 6), one of the highest values for all-polymer solar cells.[181]

Enhancing the electron deficiency of Qx with dicarboxyimide substituents lowers the HOMO of the polymer **98** to −5.47 eV, without halogen substitution on the BDT moiety (*cf.* −5.41 eV for **95**)[182] The PCE of 18.8% achieved in all-polymer cells with the **PY-IT** acceptor stands as the record value for non-halogenated polymer donors.

BDT copolymers with other acceptors

A number of other, less common acceptors that have been used for high-performing BDT-based polymers including benzimidazole-fused dithiophene, pentacyclic azepinedione, *etc.*[183–185] Copolymer **99** (Fig. 14 and Table 6) with difluorobenzothiazole has a wide bandgap of 2.06 eV.[186] Devices with **99** achieved high performance with several NFAs, among which the **99 : L8-BO** mixture delivered a PCE of 18.6%. Benzobisthiazole is a stronger acceptor unit than difluorobenzothiazole endowing polymer **100** with a fairly low HOMO of −5.66 eV (*cf.* −5.43 eV for **99**).[187] Interestingly, the **100 : Y6** BHJ showed a respectable PCE of 15.1% despite the energy offset between **100** and **Y6** being only 0.04 V, significantly below the commonly recommended >0.3 eV. A derivative of **100** with different alkyl chains (**101**) was later combined with the **PY-IT** acceptor and yielded a PCE of 17.2%.[188] Related polymers **102–104** were developed by connecting benzobisthiazole *via* 2,6-positions and attaching additional alkylthienyl side chains to the 4,8-positions.[189,190] This acceptor unit is isoelectronic to the dithienyl-BDT donor unit and the expanded side-chain conjugation contributes to the redshifted absorptions for **102–104**. Introducing **102–104** as the third component in a ternary BHJ enhances the absorption of the active layer, resulting in PCEs of 17.9–19.0%.

The large fused polycyclic structure of the thienoacenaphthylenedicarboxyimide acceptor in polymer **105** results in its low solubility in chloroform. Thus, films of **105** cast from chlorobenzene can tolerate the chloroform deposition of the **N3** acceptor during bilayer device fabrication.[191] The resulting bilayer films achieved PCEs as high as 17.6% and showed very little batch-to-batch variation, even for polymers of different molecular weights, which is critical for commercial applications. **106** with the difluoronaphthodithiophene acceptor presents a higher HOMO and wider bandgap compared to its analog **75** (**D18**), due to the relatively low electron deficiency of difluoronaphthodithiophene.[192] OPV devices with the **106 : BTP-eC9** blend yielded a PCE of 16.2%. Although this is no longer a record-breaking efficiency, it is worth noting that the difluoronaphthodithiophene unit can be synthesized in two steps in >70% yield, which compares favorably to the four-step <30% yield synthesis of the DTBT monomer of **D18**.

In recent years, developing low-cost polymer donors incorporating simple acceptor units has become an important trend. Many of the champion materials discussed above are based on sophisticated acceptor comonomers which require as many as 17 synthetic steps (!) and complex purification in their preparation.[54,64,168] In contrast, polymer **107** used a simple acceptor, 1,3,4-thiadiazole.[193] **107** has a wide bandgap of 2.12 eV and an ultra-deep HOMO level of −5.64 eV. This low HOMO contributes to the high V_{OC} of 0.96 V in a BHJ with **IT-4F**, and the corresponding device reached a PCE of 14.5%. **108** was built by copolymerizing BDT with cyanoterthiophene, which can be prepared in 3 synthetic steps.[194] The OPV devices of **108** with **Y6** achieved high PCE in the range of 15.9–17.1%. Notably, the molecular weight of this polymer (M_n ranging from 18 to 74 kDa) showed very little effect on the device efficiency, which is important for batch-to-batch reproducibility. Another simple acceptor, 4-chlorothiazole, was used to synthesize polymer **109**.[195] **109** delivered a PCE of 15.0% in a binary device with **BTP-eC9-4F** and 19.2% in a ternary system with **75** and **L8-BO**, outperforming current benchmark polymer donors (**PM6**, **D18**, *etc.*) in terms of ratio of PCE to synthetic complexity.

1,2,3-Benzothiadiazole (iBT), an asymmetric isomer of BT which can be readily made in one step from 2-mercaptoaniline, was used as an acceptor in polymer **110**.[196] The absorption band of **110** is blue-shifted compared to its BT analog, indicating a lower electron-deficiency of iBT *vs.* BT unit. On the other hand, single-crystal X-ray analysis of methylthiophene-iBT and methylthiophene-BT shows that the iBT unit provides a more planar connection with the adjacent thiophene linkers, which could explain a two-fold increase of charge carrier mobility of **110** to 2.3×10^{-3} cm^2 V^{-1} s^{-1}. The device with **110** and **Y6** achieved a PCE of 19.0% with a high J_{SC} of 28.2 mA cm^{-2}. This is a remarkable efficiency for the binary **Y6**-only device which shows that there is room for improving the performance of BDT polymers beyond the classical **PM6** and **D18** structures.

Conclusions and outlook

Over the past decades, great research efforts have been invested in the design of semiconducting polymer donors for OPVs. In particular, several hundreds of BDT-based copolymers were investigated as OPV materials. Molecular engineering of the conjugated backbone, as well as side chain engineering, have been effective in developing p-type polymer semiconductors with controlled bandgap, good charge transport properties and processability. With these strategies, bandgaps between 1.3 and 2.1 eV and hole mobility as high as 8.6×10^{-3} cm^2 V^{-1} s^{-1} have been realized. As a result, PCEs exceeding 20% have been reliably achieved for small-area devices[148,197] and 13.9% for a 55 cm^2 sub-module processed in green solvents.[198] Nevertheless, the broad deployment of BDT-based polymers in the commercialization of OPV technology still requires solving a number of issues.

Morphological control, now well-understood for BHJs based on P3HT and fullerene derivatives,[199] remains difficult for high-performing BDT polymers and requires exploring new approaches. For example, matching the solution aggregation of donors and acceptors can favor the formation of an optimal device morphology, crucial for achieving high PCE.[200] BDT-based polymers offer opportunities to create a diverse range of polymers with varying aggregation properties, influenced by molecular confirmation and interchain stacking, *via* modifications to side chains, substituents positions, *etc.* In this context, quasi-planar heterojunctions prepared by sequential solution

coating of the BDT polymer donor and the NFA layers, can now deliver OPVs with very high PCE, and potentially are easier to control than BHJs.[201]

At the molecular level, a few sub-classes of BDT-based donor–acceptor polymers have emerged as champions of high-performance OPVs. Most of these are based on either benzodithiophenedione (**PBDB-T**, **PM6**, **PM7** are their variations) or dithienobenzothiadiazole (**D18** and variations) acceptor units. While the search for alternative structures with high OPV performance takes place worldwide, it is important to remember that increased chemical complexity comes at a cost and ultimately the simpler structures are more likely to lead to a commercially successful technology.

Given the lengthy synthesis of the BDT-based (and most other high-performing) polymers, more attention should be paid to developing environmentally friendly synthetic routes with fewer steps, such as DArP. The side chains commonly placed at the 4,8-positions of BDT create the steric hindrance of the β-CH, improving the regioselectivity of DArP to the α-CH positions. However, still relatively few papers explore the DArP copolymerization of BDT with other building blocks.[37,202,203] Further research establishing the optimal reaction conditions is necessary for the broader implementation of this strategy.

The role of computational chemistry in material development has significantly increased over the past decade, aiding in understanding the structure–property relationships, reducing the workload in screening experiments and design of new, highly complex materials.[204] However, most simulations of conjugated materials (including BDT-based polymers) have relied on density-functional theory calculations of individual molecules or single polymer chains (under periodic boundary conditions). While these calculations may accurately represent the molecular properties (confirmation, orbital/band energies, *etc.*), they give only limited insights into the behavior of such molecules in the condensed phase, especially in heterogeneous semicrystalline bulk heterojunction films. Multiscale modeling of the latter is an infinitely more difficult problem, and most attempts have focused on the simple (and likely no longer technologically relevant) model polymers such as P3HT.[205–207] Advancing such modeling of the key parameters of OPV active layers such as phase separation, exciton dissociation/recombination, and charge mobilities is essential for the progress of the field. While machine learning is becoming an increasingly valuable tool in the OPV field,[204,208–210] its application in designing BDT-based polymer donors and actively predicting the behaviour of such materials in devices is yet to be fully explored.

Last but not least, while the high (photo)stability of the BDT building block is one of the reasons for its widespread application in OPV materials, the stability of BDT-containing polymers can vary widely with its structure. Although a correlation between the energy levels of the polymer and its resistance to photooxidation has been demonstrated in some cases,[211–213] it is also clear that the redox properties are not sufficient to predict the photostability.[214] A better understanding of the photodegradation pathways of BDT polymers is required for designing more stable solar cells.

Abbreviations

A	Acceptor
BDD	Benzo[1,2-*c*:4,5-*c*′]dithiophene-4,8-dione
BDT	Benzo[1,2-*b*:4,5-*b*′]dithiophene
BHJ	Bulk heterojunction
BT	Benzo[*c*][1,2,5]thiadiazole
BTz	Benzo[*d*][1,2,3]triazole
D	Donor
DArP	Direct C–H arylation polymerization
DPP	Diketopyrrolopyrrole
DTBT	Dithienobenzothiadiazole
FF	Fill factor
GIXS	Grazing-incidence X-ray scattering
HOMO	Highest occupied molecular orbital
J_{SC}	Short-circuit current density
LUMO	Lowest unoccupied molecular orbital
NFA	Non-fullerene acceptor
OPV	Organic photovoltaics
PCE	Power conversion efficiency
$PC_{61}BM$	(6,6)-Phenyl-C_{61}-butyric acid methyl ester
$PC_{71}BM$	(6,6)-Phenyl-C_{71}-butyric acid methyl ester
P3HT	Poly(3-hexylthiophene)
Qx	Quinoxaline
TT	Thieno[3,4-*b*]thiophene
V_{OC}	Open-circuit voltage

Data availability

No primary research results, software or code have been included and no new data were generated or analysed as part of this review.

Conflicts of interest

There are no conflicts to declare.

Acknowledgements

This work was supported by NSERC Discovery and NRC AI4D grants. The authors thank Dr Steven Xiao (1-Material Inc) and Dr Jianping Lu (NRC) for useful discussions.

Notes and references

1 C. W. Tang, *Appl. Phys. Lett.*, 1986, **48**, 183–185.
2 J. J. M. Halls, C. A. Walsh, N. C. Greenham, E. A. Marseglia, R. H. Friend, S. C. Moratti and A. B. Holmes, *Nature*, 1995, **376**, 498–500.
3 G. Yu, J. Gao, J. C. Hummelen, F. Wudl and A. J. Heeger, *Science*, 1995, **270**, 1789–1791.
4 F. Padinger, R. S. Rittberger and N. S. Sariciftci, *Adv. Funct. Mater.*, 2003, **13**, 85–88.

5 G. Li, V. Shrotriya, J. Huang, Y. Yao, T. Moriarty, K. Emery and Y. Yang, *Nat. Mater.*, 2005, **4**, 864–868.
6 Y. Kim, S. Cook, S. M. Tuladhar, S. A. Choulis, J. Nelson, J. R. Durrant, D. D. C. Bradley, M. Giles, I. McCulloch, C.-S. Ha and M. Ree, *Nat. Mater.*, 2006, **5**, 197–203.
7 J. Roncali, *Chem. Rev.*, 1997, **97**, 173–206.
8 J. Wang, P. Xue, Y. Jiang, Y. Huo and X. Zhan, *Nat. Rev. Chem.*, 2022, **6**, 614–634.
9 M. Svensson, F. Zhang, S. C. Veenstra, W. J. H. Verhees, J. C. Hummelen, J. M. Kroon, O. Inganäs and M. R. Andersson, *Adv. Mater.*, 2003, **15**, 988–991.
10 M. Zhang, H. N. Tsao, W. Pisula, C. Yang, A. K. Mishra and K. Müllen, *J. Am. Chem. Soc.*, 2007, **129**, 3472–3473.
11 N. Blouin, A. Michaud and M. Leclerc, *Adv. Mater.*, 2007, **19**, 2295–2300.
12 R. S. Loewe, S. M. Khersonsky and R. D. McCullough, *Adv. Mater.*, 1999, **11**, 250–253.
13 D. W. H. MacDowell and J. C. Wisowaty, *J. Org. Chem.*, 1971, **36**, 4004–4012.
14 M. Pomerantz, J. Wang, S. Seong, K. P. Starkey, L. Nguyen and D. S. Marynick, *Macromolecules*, 1994, **27**, 7478–7485.
15 J. Hou, M.-H. Park, S. Zhang, Y. Yao, L.-M. Chen, J.-H. Li and Y. Yang, *Macromolecules*, 2008, **41**, 6012–6018.
16 Y.-J. Cheng, S.-H. Yang and C.-S. Hsu, *Chem. Rev.*, 2009, **109**, 5868–5923.
17 C. Duan, F. Huang and Y. Cao, *J. Mater. Chem.*, 2012, **22**, 10416–10434.
18 L. Ye, S. Zhang, L. Huo, M. Zhang and J. Hou, *Acc. Chem. Res.*, 2014, **47**, 1595–1603.
19 C. Cui and Y. Li, *Energy Environ. Sci.*, 2019, **12**, 3225–3246.
20 B. Zheng, L. Huo and Y. Li, *NPG Asia Mater.*, 2020, **12**, 3.
21 H. Yao, L. Ye, H. Zhang, S. Li, S. Zhang and J. Hou, *Chem. Rev.*, 2016, **116**, 7397–7457.
22 C. Lin, R. Peng, J. Shi and Z. Ge, *Exploration*, 2024, **4**, 20230122.
23 Y. Wei, Q. Peng, C. Zhong, S. Ma, T. Wang, Y. Pu, W. Zhang, S. Wang and L. Xie, *Dyes Pigm.*, 2024, **225**, 112097.
24 D. Zhou, Y. Wang, S. Yang, J. Quan, J. Deng, J. Wang, Y. Li, Y. Tong, Q. Wang and L. Chen, *Small*, 2024, **20**, 2306854.
25 C. An and J. Hou, *Acc. Mater. Res.*, 2022, **3**, 540–551.
26 D. Cevher, S. C. Cevher and A. Cirpan, *Mater. Today Commun.*, 2023, **37**, 107524.
27 D. Lee, S. W. Stone and J. P. Ferraris, *Chem. Commun.*, 2011, **47**, 10987–10989.
28 R. L. Uy, L. Yan, W. Li and W. You, *Macromolecules*, 2014, **47**, 2289–2295.
29 H. Pan, Y. Li, Y. Wu, P. Liu, B. S. Ong, S. Zhu and G. Xu, *Chem. Mater.*, 2006, **18**, 3237–3241.
30 T. M. Pappenfus, D. T. Seidenkranz and E. W. Reinheimer, *Heterocycles*, 2012, **85**, 355–364.
31 D. Liu, Q. Zhu, C. Gu, J. Wang, M. Qiu, W. Chen, X. Bao, M. Sun and R. Yang, *Adv. Mater.*, 2016, **28**, 8490–8498.
32 S. Sharma, R. Soni, S. Kurungot and S. K. Asha, *J. Phys. Chem. C*, 2019, **123**, 2084–2093.
33 P. A. Cox, M. Reid, A. G. Leach, A. D. Campbell, E. J. King and G. C. Lloyd-Jones, *J. Am. Chem. Soc.*, 2017, **139**, 13156–13165.
34 Z. Xiao, J. Subbiah, K. Sun, D. J. Jones, A. B. Holmes and W. W. H. Wong, *Polym. Chem.*, 2014, **5**, 6710–6717.
35 D. Zhou, N. Y. Doumon, M. Abdu-Aguye, D. Bartesaghi, M. A. Loi, L. J. Anton Koster, R. C. Chiechi and J. C. Hummelen, *RSC Adv.*, 2017, **7**, 27762–27769.
36 R. Matsidik, H. Komber, A. Luzio, M. Caironi and M. Sommer, *J. Am. Chem. Soc.*, 2015, **137**, 6705–6711.
37 A. S. Dudnik, T. J. Aldrich, N. D. Eastham, R. P. H. Chang, A. Facchetti and T. J. Marks, *J. Am. Chem. Soc.*, 2016, **138**, 15699–15709.
38 L. G. Mercier and M. Leclerc, *Acc. Chem. Res.*, 2013, **46**, 1597–1605.
39 D. Zimmermann, C. Sprau, J. Schröder, V. G. Gregoriou, A. Avgeropoulos, C. L. Chochos, A. Colsmann, S. Janietz and H. Krüger, *J. Polym. Sci., Part A: Polym. Chem.*, 2018, **56**, 1457–1467.
40 F. Lombeck, H. Komber, S. I. Gorelsky and M. Sommer, *ACS Macro Lett.*, 2014, **3**, 819–823.
41 A. E. Rudenko and B. C. Thompson, *J. Polym. Sci., Part A: Polym. Chem.*, 2015, **53**, 135–147.
42 J. Kuwabara, Y. Fujie, K. Maruyama, T. Yasuda and T. Kanbara, *Macromolecules*, 2016, **49**, 9388–9395.
43 M. Shi, T. Wang, Y. Wu, R. Sun, W. Wang, J. Guo, Q. Wu, W. Yang and J. Min, *Adv. Energy Mater.*, 2021, **11**, 2002709.
44 Y. He, L. Huo and B. Zheng, *Nano Energy*, 2024, **123**, 109397.
45 S. Smeets, Q. Liu, J. Vanderspikken, T. J. Quill, S. Gielen, L. Lutsen, K. Vandewal and W. Maes, *Chem. Mater.*, 2023, **35**, 8158–8169.
46 C. K. Lo, R. M. W. Wolfe and J. R. Reynolds, *Chem. Mater.*, 2021, **33**, 4842–4852.
47 J. A. Schneider and D. F. Perepichka, in *Adv. Mater.*, ed. T. van de Ven and S. Armand, De Gruyter, Berlin, Boston, 2020, pp. 1–50, DOI: **10.1515/9783110537734-001**.
48 L. Huo, J. Hou, H.-Y. Chen, S. Zhang, Y. Jiang, T. L. Chen and Y. Yang, *Macromolecules*, 2009, **42**, 6564–6571.
49 Y. Liang, Y. Wu, D. Feng, S.-T. Tsai, H.-J. Son, G. Li and L. Yu, *J. Am. Chem. Soc.*, 2009, **131**, 56–57.
50 C.-Y. Mei, L. Liang, F.-G. Zhao, J.-T. Wang, L.-F. Yu, Y.-X. Li and W.-S. Li, *Macromolecules*, 2013, **46**, 7920–7931.
51 E. Zhou, J. Cong, K. Hashimoto and K. Tajima, *Macromolecules*, 2013, **46**, 763–768.
52 Z. Zhang, B. Peng, B. Liu, C. Pan, Y. Li, Y. He, K. Zhou and Y. Zou, *Polym. Chem.*, 2010, **1**, 1441–1447.
53 Y. Ie, J. Huang, Y. Uetani, M. Karakawa and Y. Aso, *Macromolecules*, 2012, **45**, 4564–4571.
54 D. Qian, L. Ye, M. Zhang, Y. Liang, L. Li, Y. Huang, X. Guo, S. Zhang, Z. a. Tan and J. Hou, *Macromolecules*, 2012, **45**, 9611–9617.
55 L. Xu, S. Li, W. Zhao, Y. Xiong, J. Yu, J. Qin, G. Wang, R. Zhang, T. Zhang, Z. Mu, J. Zhao, Y. Zhang, S. Zhang, V. Kuvondikov, E. Zakhidov, Q. Peng, N. Wang, G. Xing, F. Gao, J. Hou, W. Huang and J. Wang, *Adv. Mater.*, 2024, 2403476.
56 H. J. Son, W. Wang, T. Xu, Y. Liang, Y. Wu, G. Li and L. Yu, *J. Am. Chem. Soc.*, 2011, **133**, 1885–1894.

57 A. Najari, S. Beaupré, P. Berrouard, Y. Zou, J.-R. Pouliot, C. Lepage-Pérusse and M. Leclerc, *Adv. Funct. Mater.*, 2011, **21**, 718–728.
58 R. Duan, L. Ye, X. Guo, Y. Huang, P. Wang, S. Zhang, J. Zhang, L. Huo and J. Hou, *Macromolecules*, 2012, **45**, 3032–3038.
59 X. Wang, Y. Sun, S. Chen, X. Guo, M. Zhang, X. Li, Y. Li and H. Wang, *Macromolecules*, 2012, **45**, 1208–1216.
60 P. Ding, Y. Zou, C.-C. Chu, D. Xiao and C.-S. Hsu, *J. Appl. Polym. Sci.*, 2012, **125**, 3936–3945.
61 H.-Y. Chen, S.-C. Yeh, C.-T. Chen and C.-T. Chen, *J. Mater. Chem.*, 2012, **22**, 21549–21559.
62 L. Mohammad, Q. Chen, A. Mitul, J. Sun, D. Khatiwada, B. Vaagensmith, C. Zhang, J. Li and Q. Qiao, *J. Phys. Chem. C*, 2015, **119**, 18992–19000.
63 Z. Fei, F. D. Eisner, X. Jiao, M. Azzouzi, J. A. Röhr, Y. Han, M. Shahid, A. S. R. Chesman, C. D. Easton, C. R. McNeill, T. D. Anthopoulos, J. Nelson and M. Heeney, *Adv. Mater.*, 2018, **30**, 1705209.
64 B. Fan, M. Li, D. Zhang, W. Zhong, L. Ying, Z. Zeng, K. An, Z. Huang, L. Shi, G. C. Bazan, F. Huang and Y. Cao, *ACS Energy Lett.*, 2020, **5**, 2087–2094.
65 Y. Wu, C. An, L. Shi, L. Yang, Y. Qin, N. Liang, C. He, Z. Wang and J. Hou, *Angew. Chem., Int. Ed.*, 2018, **57**, 12911–12915.
66 S. Chen, Y. Liu, L. Zhang, P. C. Y. Chow, Z. Wang, G. Zhang, W. Ma and H. Yan, *J. Am. Chem. Soc.*, 2017, **139**, 6298–6301.
67 H. Bin, Z.-G. Zhang, L. Gao, S. Chen, L. Zhong, L. Xue, C. Yang and Y. Li, *J. Am. Chem. Soc.*, 2016, **138**, 4657–4664.
68 Y. Wu, Z. Li, W. Ma, Y. Huang, L. Huo, X. Guo, M. Zhang, H. Ade and J. Hou, *Adv. Mater.*, 2013, **25**, 3449–3455.
69 M. Du, A. Tang, J. Yu, Y. Geng, Z. Wang, Q. Guo, Y. Zhong, S. Lu and E. Zhou, *Adv. Energy Mater.*, 2023, **13**, 2302429.
70 L. Huo, X. Guo, Y. Li and J. Hou, *Chem. Commun.*, 2011, **47**, 8850–8852.
71 J. Hou, H.-Y. Chen, S. Zhang, R. I. Chen, Y. Yang, Y. Wu and G. Li, *J. Am. Chem. Soc.*, 2009, **131**, 15586–15587.
72 J. Yi, M. Pan, L. Chen, Y. Chen, I. C. Angunawela, S. Luo, T. Zhang, A. Zeng, J. Chen, Z. Qi, H. Yu, W. Liu, J. Y. L. Lai, H. K. Kim, X. Zhu, H. Ade, H. Lin and H. Yan, *Adv. Energy Mater.*, 2022, **12**, 2201850.
73 T. E. Kang, K.-H. Kim and B. J. Kim, *J. Mater. Chem. A*, 2014, **2**, 15252–15267.
74 M.-C. Yuan, M.-Y. Chiu, C.-M. Chiang and K.-H. Wei, *Macromolecules*, 2010, **43**, 6270–6277.
75 Y. Huang, M. Zhang, H. Chen, F. Wu, Z. Cao, L. Zhang and S. Tan, *J. Mater. Chem. A*, 2014, **2**, 5218–5223.
76 H. Heo, H. Kim, D. Lee, S. Jang, L. Ban, B. Lim, J. Lee and Y. Lee, *Macromolecules*, 2016, **49**, 3328–3335.
77 L. Huo and J. Hou, *Polym. Chem.*, 2011, **2**, 2453–2461.
78 P. Sista, M. C. Biewer and M. C. Stefan, *Macromol. Rapid Commun.*, 2012, **33**, 9–20.
79 Y. Liang, Z. Xu, J. Xia, S.-T. Tsai, Y. Wu, G. Li, C. Ray and L. Yu, *Adv. Mater.*, 2010, **22**, E135–E138.
80 C. Cabanetos, A. El Labban, J. A. Bartelt, J. D. Douglas, W. R. Mateker, J. M. J. Fréchet, M. D. McGehee and P. M. Beaujuge, *J. Am. Chem. Soc.*, 2013, **135**, 4656–4659.
81 Y. Li and Y. Zou, *Adv. Mater.*, 2008, **20**, 2952–2958.
82 C. Bathula, C. E. Song, S. Badgujar, S.-J. Hong, I.-N. Kang, S.-J. Moon, J. Lee, S. Cho, H.-K. Shim and S. K. Lee, *J. Mater. Chem.*, 2012, **22**, 22224–22232.
83 S. Wen, X. Yun, W. Chen, Q. Liu, D. Zhu, C. Gu, M. Sun and R. Yang, *RSC Adv.*, 2014, **4**, 58426–58431.
84 L. Huo, J. Hou, S. Zhang, H.-Y. Chen and Y. Yang, *Angew. Chem., Int. Ed.*, 2010, **49**, 1500–1503.
85 S.-H. Liao, H.-J. Jhuo, Y.-S. Cheng and S.-A. Chen, *Adv. Mater.*, 2013, **25**, 4766–4771.
86 R. Sheng, Q. Liu, W. Chen, M. Sun, H. Zheng, J. Ren and R. Yang, *J. Polym. Sci., Part A: Polym. Chem.*, 2016, **54**, 1615–1622.
87 S. Zhang, L. Ye, W. Zhao, D. Liu, H. Yao and J. Hou, *Macromolecules*, 2014, **47**, 4653–4659.
88 K. Ma, H. Liang, Y. Wang, X. Jia, W. Shi, Z. Yao, X. Wan, C. Li and Y. Chen, *Macromolecules*, 2024, **57**, 8392–8400.
89 M. Zhang, X. Guo, W. Ma, H. Ade and J. Hou, *Adv. Mater.*, 2015, **27**, 4655–4660.
90 H. W. Cho, S. Y. Jeong, Z. Wu, H. Lim, W.-W. Park, W. Lee, J. V. Suman Krishna, O.-H. Kwon, J. Y. Kim and H. Y. Woo, *J. Mater. Chem. A*, 2023, **11**, 7053–7065.
91 S. Zhang, Y. Qin, J. Zhu and J. Hou, *Adv. Mater.*, 2018, **30**, 1800868.
92 Z. Li, Y. Ma and Q. Zheng, *J. Mater. Chem. A*, 2023, **11**, 5127–5134.
93 C. Cui, W.-Y. Wong and Y. Li, *Energy Environ. Sci.*, 2014, **7**, 2276–2284.
94 H. Yao, H. Zhang, L. Ye, W. Zhao, S. Zhang and J. Hou, *ACS Appl. Mater. Interfaces*, 2016, **8**, 3575–3583.
95 H. Bin, L. Gao, Z.-G. Zhang, Y. Yang, Y. Zhang, C. Zhang, S. Chen, L. Xue, C. Yang, M. Xiao and Y. Li, *Nat. Commun.*, 2016, **7**, 13651.
96 H. Bin, Y. Yang, Z. Peng, L. Ye, J. Yao, L. Zhong, C. Sun, L. Gao, H. Huang, X. Li, B. Qiu, L. Xue, Z.-G. Zhang, H. Ade and Y. Li, *Adv. Energy Mater.*, 2018, **8**, 1702324.
97 T. Qin, W. Zajaczkowski, W. Pisula, M. Baumgarten, M. Chen, M. Gao, G. Wilson, C. D. Easton, K. Müllen and S. E. Watkins, *J. Am. Chem. Soc.*, 2014, **136**, 6049–6055.
98 W. Zhao, D. Qian, S. Zhang, S. Li, O. Inganäs, F. Gao and J. Hou, *Adv. Mater.*, 2016, **28**, 4734–4739.
99 C.-M. Hsieh, M.-R. Chuang, Y. Yamada, C.-J. Su, Y. J. Chang, M. Murata, U. S. Jeng and S.-C. Chuang, *ACS Appl. Mater. Interfaces*, 2021, **13**, 61473–61486.
100 X. Wang, H. Lu, Y. Liu, A. Zhang, N. Yu, H. Wang, S. Li, Y. Zhou, X. Xu, Z. Tang and Z. Bo, *Adv. Energy Mater.*, 2021, **11**, 2102591.
101 Y. Zhou, M. Li, H. Lu, H. Jin, X. Wang, Y. Zhang, S. Shen, Z. Ma, J. Song and Z. Bo, *Adv. Funct. Mater.*, 2021, **31**, 2101742.
102 J. Zhou, Z. He, Y. Sun, A. Tang, Q. Guo and E. Zhou, *ACS Appl. Mater. Interfaces*, 2022, **14**, 41296–41303.
103 Y. Che, M. R. Niazi, Q. Chan, P. Ghamari, T. Yu, C. Ruchlin, H. Yu, H. Yan, D. Ma, S. S. Xiao, R. Izquierdo and D. F. Perepichka, *Angew. Chem., Int. Ed.*, 2023, **62**, e202309003.

104 H. Lu, W. Liu, H. Jin, H. Huang, Z. Tang and Z. Bo, *Adv. Funct. Mater.*, 2022, **32**, 2107756.
105 H. Zhao, Z. Yin, P. Gu, Y. Liu, W. Wang, H. Lai, H.-Q. Wang, N. Li and W. Song, *ACS Appl. Energy Mater.*, 2023, **6**, 1595–1604.
106 J. Yuan, Y. Zhang, L. Zhou, G. Zhang, H.-L. Yip, T.-K. Lau, X. Lu, C. Zhu, H. Peng, P. A. Johnson, M. Leclerc, Y. Cao, J. Ulanski, Y. Li and Y. Zou, *Joule*, 2019, **3**, 1140–1151.
107 L. Ma, S. Zhang, J. Zhu, J. Wang, J. Ren, J. Zhang and J. Hou, *Nat. Commun.*, 2021, **12**, 5093.
108 L. Zhu, M. Zhang, J. Xu, C. Li, J. Yan, G. Zhou, W. Zhong, T. Hao, J. Song, X. Xue, Z. Zhou, R. Zeng, H. Zhu, C.-C. Chen, R. C. I. MacKenzie, Y. Zou, J. Nelson, Y. Zhang, Y. Sun and F. Liu, *Nat. Mater.*, 2022, **21**, 656–663.
109 X. Yu, P. Ding, D. Yang, P. Yan, H. Wang, S. Yang, J. Wu, Z. Wang, H. Sun, Z. Chen, L. Xie and Z. Ge, *Angew. Chem., Int. Ed.*, 2024, **63**, e202401518.
110 S. Li, L. Zhan, Y. Jin, G. Zhou, T.-K. Lau, R. Qin, M. Shi, C.-Z. Li, H. Zhu, X. Lu, F. Zhang and H. Chen, *Adv. Mater.*, 2020, **32**, 2001160.
111 T. Duan, W. Feng, Y. Li, Z. Li, Z. Zhang, H. Liang, H. Chen, C. Zhong, S. Jeong, C. Yang, S. Chen, S. Lu, O. A. Rakitin, C. Li, X. Wan, B. Kan and Y. Chen, *Angew. Chem., Int. Ed.*, 2023, **62**, e202308832.
112 S. Ono, T. Mikie, K. Nakano, K. Tajima and I. Osaka, *ACS Appl. Energy Mater.*, 2024, **7**, 2946–2954.
113 R. Zhang, H. Chen, T. Wang, L. Kobera, L. He, Y. Huang, J. Ding, B. Zhang, A. Khasbaatar, S. Nanayakkara, J. Zheng, W. Chen, Y. Diao, S. Abbrent, J. Brus, A. H. Coffey, C. Zhu, H. Liu, X. Lu, Q. Jiang, V. Coropceanu, J.-L. Brédas, Y. Li, Y. Li and F. Gao, *Nat. Energy*, 2024, **10**, 124–134.
114 J. Grüne, G. Londi, A. J. Gillett, B. Stähly, S. Lulei, M. Kotova, Y. Olivier, V. Dyakonov and A. Sperlich, *Adv. Funct. Mater.*, 2023, **33**, 2212640.
115 J. Li, Q. Ji, R. Wang, Z.-G. Zhang, X. Wang, M. Xiao, Y.-q. Lu and C. Zhang, *J. Am. Chem. Soc.*, 2024, **146**, 20312–20322.
116 K. Li, Q. Fan, Y. Guo, Z. Wei, X. Yu, J. Zhong and J. Huang, *Adv. Opt. Mater.*, 2023, **11**, 2203040.
117 C. Guan, C. Xiao, X. Liu, Z. Hu, R. Wang, C. Wang, C. Xie, Z. Cai and W. Li, *Angew. Chem., Int. Ed.*, 2023, **62**, e202312357.
118 X. Li, H. Ke, S. Li, M. Gao, S. Li, J. Yu, H. Xie, K. Zhou, K. Zhang and L. Ye, *Adv. Funct. Mater.*, 2024, **34**, 2400702.
119 R. Sun, Q. Wu, J. Guo, T. Wang, Y. Wu, B. Qiu, Z. Luo, W. Yang, Z. Hu, J. Guo, M. Shi, C. Yang, F. Huang, Y. Li and J. Min, *Joule*, 2020, **4**, 407–419.
120 J. Yu, X. Liu, Z. Zhong, C. Yan, H. Liu, P. W. K. Fong, Q. Liang, X. Lu and G. Li, *Nano Energy*, 2022, **94**, 106923.
121 M.-A. Pan, T.-K. Lau, Y. Tang, Y.-C. Wu, T. Liu, K. Li, M.-C. Chen, X. Lu, W. Ma and C. Zhan, *J. Mater. Chem. A*, 2019, **7**, 20713–20722.
122 Q. Guo, R. Ma, J. Hu, Z. Wang, H. Sun, X. Dong, Z. Luo, T. Liu, X. Guo, X. Guo, H. Yan, F. Liu and M. Zhang, *Adv. Funct. Mater.*, 2020, **30**, 2000383.
123 G. Li, D. Li, R. Ma, T. Liu, Z. Luo, G. Cui, L. Tong, M. Zhang, Z. Wang, F. Liu, L. Xu, H. Yan and B. Tang, *J. Mater. Chem. A*, 2020, **8**, 5927–5935.
124 Z. He, S. Li, R. Zeng, Y. Lin, Y. Zhang, Z. Hao, S. Zhang, F. Liu, Z. Tang and H. Zhong, *Adv. Mater.*, 2404824.
125 H. Sun, T. Liu, J. Yu, T.-K. Lau, G. Zhang, Y. Zhang, M. Su, Y. Tang, R. Ma, B. Liu, J. Liang, K. Feng, X. Lu, X. Guo, F. Gao and H. Yan, *Energy Environ. Sci.*, 2019, **12**, 3328–3337.
126 J. Liang, M. Pan, G. Chai, Z. Peng, J. Zhang, S. Luo, Q. Han, Y. Chen, A. Shang, F. Bai, Y. Xu, H. Yu, J. Y. L. Lai, Q. Chen, M. Zhang, H. Ade and H. Yan, *Adv. Mater.*, 2020, **32**, 2003500.
127 X. Guo, Q. Fan, J. Wu, G. Li, Z. Peng, W. Su, J. Lin, L. Hou, Y. Qin, H. Ade, L. Ye, M. Zhang and Y. Li, *Angew. Chem., Int. Ed.*, 2021, **60**, 2322–2329.
128 H. Lu, H. Wang, G. Ran, S. Li, J. Zhang, Y. Liu, W. Zhang, X. Xu and Z. Bo, *Adv. Funct. Mater.*, 2022, **32**, 2203193.
129 J. Wu, G. Li, J. Fang, X. Guo, L. Zhu, B. Guo, Y. Wang, G. Zhang, L. Arunagiri, F. Liu, H. Yan, M. Zhang and Y. Li, *Nat. Commun.*, 2020, **11**, 4612.
130 R. Sun, Y. Wu, X. Yang, Y. Gao, Z. Chen, K. Li, J. Qiao, T. Wang, J. Guo, C. Liu, X. Hao, H. Zhu and J. Min, *Adv. Mater.*, 2022, **34**, 2110147.
131 Z. U. Rehman, M. Haris, S. U. Ryu, M. Jahankhan, C. E. Song, H. K. Lee, S. K. Lee, W. S. Shin, T. Park and J.-C. Lee, *Adv. Sci.*, 2023, **10**, 2302376.
132 B. Pang, C. Liao, X. Xu, S. Peng, J. Xia, Y. Guo, Y. Xie, Y. Chen, C. Duan, H. Wu, R. Li and Q. Peng, *Adv. Mater.*, 2023, **35**, 2211871.
133 S. Hao, X. Xu, L. Yu, S. Peng, J. Xia, Y. Xie, C. Duan, H. Wu, R. Li and Q. Peng, *Adv. Mater.*, 2023, **35**, 2301732.
134 J.-W. Lee, C. Lim, S.-W. Lee, Y. Jeon, S. Lee, T.-S. Kim, J.-Y. Lee and B. J. Kim, *Adv. Energy Mater.*, 2022, **12**, 2202224.
135 F. Cheng, Y. Cui, F. Ding, Z. Chen, Q. Xie, X. Xia, P. Zhu, X. Lu, H. Zhu, X. Liao and Y. Chen, *Adv. Mater.*, 2023, **35**, 2300820.
136 G. Zhang, Q. Wu, Y. Duan, W. Liu, S. Y. Jeong, H. Y. Woo, Q. Zhao and H. Zhou, *Adv. Funct. Mater.*, 2024, **34**, 2408678.
137 Z. Tao, Y. Li, W. Shen, H. Fu, Y. Ma and Q. Zheng, *J. Mater. Chem. C*, 2024, **12**, 8435–8441.
138 X. Gong, G. Li, S. Feng, L. Wu, Y. Liu, R. Hou, C. Li, X. Chen and Z. Bo, *J. Mater. Chem. C*, 2017, **5**, 937–942.
139 P. Cong, Z. Wang, Y. Geng, Y. Meng, C. Meng, L. Chen, A. Tang and E. Zhou, *Nano Energy*, 2023, **105**, 108017.
140 Q. Liu, Y. Jiang, K. Jin, J. Qin, J. Xu, W. Li, J. Xiong, J. Liu, Z. Xiao, K. Sun, S. Yang, X. Zhang and L. Ding, *Sci. Bull.*, 2020, **65**, 272–275.
141 H. Lu, W. Liu, G. Ran, Z. Liang, H. Li, N. Wei, H. Wu, Z. Ma, Y. Liu, W. Zhang, X. Xu and Z. Bo, *Angew. Chem., Int. Ed.*, 2023, **62**, e202314420.
142 W. Gao, F. Qi, Z. Peng, F. R. Lin, K. Jiang, C. Zhong, W. Kaminsky, Z. Guan, C.-S. Lee, T. J. Marks, H. Ade and A. K.-Y. Jen, *Adv. Mater.*, 2022, **34**, 2202089.

143 T. Jia, J. Zhang, K. Zhang, H. Tang, S. Dong, C.-H. Tan, X. Wang and F. Huang, *J. Mater. Chem. A*, 2021, **9**, 8975–8983.
144 G. Cai, Z. Chen, X. Xia, Y. Li, J. Wang, H. Liu, P. Sun, C. Li, R. Ma, Y. Zhou, W. Chi, J. Zhang, H. Zhu, J. Xu, H. Yan, X. Zhan and X. Lu, *Adv. Sci.*, 2022, **9**, 2200578.
145 Z. Ou, J. Qin, K. Jin, J. Zhang, L. Zhang, C. Yi, Z. Jin, Q. Song, K. Sun, J. Yang, Z. Xiao and L. Ding, *J. Mater. Chem. A*, 2022, **10**, 3314–3320.
146 S. Shen, Y. Mi, Y. Ouyang, Y. Lin, J. Deng, W. Zhang, J. Zhang, Z. Ma, C. Zhang, J. Song and Z. Bo, *Angew. Chem., Int. Ed.*, 2023, **62**, e202316495.
147 A. Zeng, X. Ma, M. Pan, Y. Chen, R. Ma, H. Zhao, J. Zhang, H. K. Kim, A. Shang, S. Luo, I. C. Angunawela, Y. Chang, Z. Qi, H. Sun, J. Y. L. Lai, H. Ade, W. Ma, F. Zhang and H. Yan, *Adv. Funct. Mater.*, 2021, **31**, 2102413.
148 L. Zhu, M. Zhang, G. Zhou, Z. Wang, W. Zhong, J. Zhuang, Z. Zhou, X. Gao, L. Kan, B. Hao, F. Han, R. Zeng, X. Xue, S. Xu, H. Jing, B. Xiao, H. Zhu, Y. Zhang and F. Liu, *Joule*, 2024, **8**, 3153–3168.
149 D. Qiu, C. Tian, H. Zhang, J. Zhang, Z. Wei and K. Lu, *Adv. Mater.*, 2313251.
150 X. Chen, C. Liao, M. Deng, X. Xu, L. Yu, R. Li and Q. Peng, *Chem. Eng. J.*, 2023, **451**, 139046.
151 D. He, J. Zhou, Y. Zhu, Y. Li, K. Wang, J. Li, J. Zhang, B. Li, Y. Lin, Y. He, C. Wang and F. Zhao, *Adv. Mater.*, 2024, **36**, 2308909.
152 Z. Liao, D. Hu, H. Tang, P. Huang, R. Singh, S. Chung, K. Cho, M. Kumar, L. Hou, Q. Chen, W. Yu, H. Chen, K. Yang, Z. Kan, F. Liu, Z. Xiao, G. Li and S. Lu, *J. Mater. Chem. A*, 2022, **10**, 7878–7887.
153 J. Min, Z.-G. Zhang, S. Zhang and Y. Li, *Chem. Mater.*, 2012, **24**, 3247–3254.
154 L. Gao, Z.-G. Zhang, H. Bin, L. Xue, Y. Yang, C. Wang, F. Liu, T. P. Russell and Y. Li, *Adv. Mater.*, 2016, **28**, 8288–8295.
155 L. Gao, Z.-G. Zhang, L. Xue, J. Min, J. Zhang, Z. Wei and Y. Li, *Adv. Mater.*, 2016, **28**, 1884–1890.
156 C. Yan, W. Wang, T.-K. Lau, K. Li, J. Wang, K. Liu, X. Lu and X. Zhan, *J. Mater. Chem. A*, 2018, **6**, 16638–16644.
157 J. Gao, R. Ming, Q. An, X. Ma, M. Zhang, J. Miao, J. Wang, C. Yang and F. Zhang, *Nano Energy*, 2019, **63**, 103888.
158 M. Hao, T. Liu, Y. Xiao, L.-K. Ma, G. Zhang, C. Zhong, Z. Chen, Z. Luo, X. Lu, H. Yan, L. Wang and C. Yang, *Chem. Mater.*, 2019, **31**, 1752–1760.
159 G. Xie, Z. Zhang, Z. Su, X. Zhang and J. Zhang, *Nano Energy*, 2020, **69**, 104447.
160 A. Tang, Q. Zhang, M. Du, G. Li, Y. Geng, J. Zhang, Z. Wei, X. Sun and E. Zhou, *Macromolecules*, 2019, **52**, 6227–6233.
161 X. Xue, B. Zheng, Y. Zhang, M. Zhang, D. Wei, F. Liu, M. Wan, J. Liu, G. Chen and L. Huo, *Adv. Energy Mater.*, 2020, **10**, 2002142.
162 J. Zhou, P. Cong, L. Chen, B. Zhang, Y. Geng, A. Tang and E. Zhou, *J. Energy Chem.*, 2021, **62**, 532–537.
163 H. Zhang, H.-E. Wang, T. Zhu, Z. Liu and L. Chen, *ACS Appl. Energy Mater.*, 2022, **5**, 5026–5035.
164 J. Zhou, P. Lei, Y. Geng, Z. He, X. Li, Q. Zeng, A. Tang and E. Zhou, *J. Mater. Chem. A*, 2022, **10**, 9869–9877.
165 Y. Chen, P. Lei, Y. Geng, T. Meng, X. Li, Q. Zeng, Q. Guo, A. Tang, Y. Zhong and E. Zhou, *Sci. China:Chem.*, 2023, **66**, 1190–1200.
166 T. Wang, R. Sun, S. Xu, J. Guo, W. Wang, J. Guo, X. Jiao, J. Wang, S. Jia, X. Zhu, Y. Li and J. Min, *J. Mater. Chem. A*, 2019, **7**, 14070–14078.
167 L. Wang, T. Wang, J. Oh, Z. Yuan, C. Yang, Y. Hu, X. Zhao and Y. Chen, *Chem. Eng. J.*, 2022, **442**, 136068.
168 L. Lan, Z. Chen, Q. Hu, L. Ying, R. Zhu, F. Liu, T. P. Russell, F. Huang and Y. Cao, *Adv. Sci.*, 2016, **3**, 1600032.
169 B. Fan, Z. Zeng, W. Zhong, L. Ying, D. Zhang, M. Li, F. Peng, N. Li, F. Huang and Y. Cao, *ACS Energy Lett.*, 2019, **4**, 2466–2472.
170 M. Du, A. Tang, J. Yu, Y. Geng, Z. Wang, Q. Guo, Y. Zhong, S. Lu and E. Zhou, *Adv. Energy Mater.*, 2023, **13**, 2302429.
171 N. Sun, M. Du, D. Zhang, J. Du, T. Du, L. Tang, Y. Zhang, Q. Guo and E. Zhou, *Chem. Eng. J.*, 2024, **499**, 155970.
172 Z. Zheng, O. M. Awartani, B. Gautam, D. Liu, Y. Qin, W. Li, A. Bataller, K. Gundogdu, H. Ade and J. Hou, *Adv. Mater.*, 2017, **29**, 1604241.
173 C. Sun, F. Pan, H. Bin, J. Zhang, L. Xue, B. Qiu, Z. Wei, Z.-G. Zhang and Y. Li, *Nat. Commun.*, 2018, **9**, 743.
174 C. Zhu, L. Meng, J. Zhang, S. Qin, W. Lai, B. Qiu, J. Yuan, Y. Wan, W. Huang and Y. Li, *Adv. Mater.*, 2021, **33**, 2100474.
175 Y. Cui, Y. Xu, H. Yao, P. Bi, L. Hong, J. Zhang, Y. Zu, T. Zhang, J. Qin, J. Ren, Z. Chen, C. He, X. Hao, Z. Wei and J. Hou, *Adv. Mater.*, 2021, **33**, 2102420.
176 Y. Xu, Y. Cui, H. Yao, T. Zhang, J. Zhang, L. Ma, J. Wang, Z. Wei and J. Hou, *Adv. Mater.*, 2021, **33**, 2101090.
177 D. Liu, W. Zhao, S. Zhang, L. Ye, Z. Zheng, Y. Cui, Y. Chen and J. Hou, *Macromolecules*, 2015, **48**, 5172–5178.
178 J. Wang, Y. Wang, P. Bi, Z. Chen, J. Qiao, J. Li, W. Wang, Z. Zheng, S. Zhang, X. Hao and J. Hou, *Adv. Mater.*, 2023, **35**, 2301583.
179 N. Yang, Y. Cui, T. Zhang, C. An, Z. Chen, Y. Xiao, Y. Yu, Y. Wang, X.-T. Hao and J. Hou, *J. Am. Chem. Soc.*, 2024, **146**, 9205–9215.
180 T. Chen, X. Zheng, D. Wang, Y. Zhu, Y. Ouyang, J. Xue, M. Wang, S. Wang, W. Ma, C. Zhang, Z. Ma, S. Li, L. Zuo and H. Chen, *Adv. Mater.*, 2024, **36**, 2308061.
181 J. Wang, Y. Cui, Y. Xu, K. Xian, P. Bi, Z. Chen, K. Zhou, L. Ma, T. Zhang, Y. Yang, Y. Zu, H. Yao, X. Hao, L. Ye and J. Hou, *Adv. Mater.*, 2022, **34**, 2205009.
182 Z. Wang, X. Wang, L. Tu, H. Wang, M. Du, T. Dai, Q. Guo, Y. Shi and E. Zhou, *Angew. Chem., Int. Ed.*, 2024, **63**, e202319755.
183 H. Yao, Y. Cui, D. Qian, C. S. Ponseca Jr, A. Honarfar, Y. Xu, J. Xin, Z. Chen, L. Hong, B. Gao, R. Yu, Y. Zu, W. Ma, P. Chabera, T. Pullerits, A. Yartsev, F. Gao and J. Hou, *J. Am. Chem. Soc.*, 2019, **141**, 7743–7750.
184 Q. He, J. Shaw, Y. Firdaus, X. Hu, B. Ding, A. V. Marsh, A. S. Dumon, Y. Han, Z. Fei, T. D. Anthopoulos, C. R. McNeill and M. Heeney, *Macromolecules*, 2023, **56**, 5825–5834.
185 D. Qiu, W. A. Memon, H. Lai, Y. Wang, H. Li, N. Zheng and F. He, *J. Phys. Chem. Lett.*, 2024, **15**, 10858–10865.

186 B. Pang, C. Liao, X. Xu, L. Yu, R. Li and Q. Peng, *Adv. Mater.*, 2023, **35**, 2300631.
187 S. Wang, Y. Tao, S. Li, X. Xia, Z. Chen, M. Shi, L. Zuo, H. Zhu, X. Lu and H. Chen, *Macromolecules*, 2021, **54**, 7862–7869.
188 P. Wu, Y. Duan, Y. Li, X. Xu, R. Li, L. Yu and Q. Peng, *Adv. Mater.*, 2024, **36**, 2306990.
189 J. Wang, C. Han, S. Wen, F. Bi, Z. Hu, Y. Li, C. Yang, X. Bao and J. Chu, *Energy Environ. Sci.*, 2023, **16**, 2327–2337.
190 S. Liu, J. Wang, S. Wen, F. Bi, Q. Zhu, C. Yang, C. Yang, J. Chu and X. Bao, *Adv. Mater.*, 2024, **36**, 2312959.
191 H. Ning, Q. Jiang, P. Han, M. Lin, G. Zhang, J. Chen, H. Chen, S. Zeng, J. Gao, J. Liu, F. He and Q. Wu, *Energy Environ. Sci.*, 2021, **14**, 5919–5928.
192 Z. Su, W. Liu, H. Song, N. Wei, J. Chen, Y. Lin, W. Zhang, X. Xu, Z. Ma, C. Li, A. Zhang, Y. Liu and Z. Bo, *ACS Appl. Polym. Mater.*, 2024, **6**, 12644–12653.
193 T. Zhang, C. An, P. Bi, Q. Lv, J. Qin, L. Hong, Y. Cui, S. Zhang and J. Hou, *Adv. Energy Mater.*, 2021, **11**, 2101705.
194 X. Yuan, Y. Zhao, T. Zhan, J. Oh, J. Zhou, J. Li, X. Wang, Z. Wang, S. Pang, P. Cai, C. Yang, Z. He, Z. Xie, C. Duan, F. Huang and Y. Cao, *Energy Environ. Sci.*, 2021, **14**, 5530–5540.
195 H. Lu, H. Wang, G. Ran, W. Liu, H. Huang, X. Jiang, Y. Liu, X. Xu and Z. Bo, *CCS Chem.*, 2024, **6**, 1757–1766.
196 T. Lin, Y. Hai, Y. Luo, L. Feng, T. Jia, J. Wu, R. Ma, T. A. Dela Peña, Y. Li, Z. Xing, M. Li, M. Wang, B. Xiao, K. S. Wong, S. Liu and G. Li, *Adv. Mater.*, 2024, **36**, 2312311.
197 S. Guan, Y. Li, C. Xu, N. Yin, C. Xu, C. Wang, M. Wang, Y. Xu, Q. Chen, D. Wang, L. Zuo and H. Chen, *Adv. Mater.*, 2024, **36**, 2400342.
198 T. Gokulnath, H. Kim, J. Lee, B. H. Cho, H.-Y. Park, J. Jee, Y. Y. Kim, K. Kranthiraja, J. Yoon and S.-H. Jin, *Adv. Energy Mater.*, 2023, **13**, 2302538.
199 S. Agbolaghi and S. Zenoozi, *Org. Electron.*, 2017, **51**, 362–403.
200 L. Xu, S. Li, W. Zhao, Y. Xiong, J. Yu, J. Qin, G. Wang, R. Zhang, T. Zhang and Z. Mu, *Adv. Mater.*, 2024, 2403476.
201 Y. Zhu and F. He, *ACS Energy Lett.*, 2025, **10**, 935–946.
202 M. Wakioka, N. Torii, M. Saito, I. Osaka and F. Ozawa, *ACS Appl. Polym. Mater.*, 2021, **3**, 830–836.
203 L.-J. Yang, N. Chen, X.-M. Huang, Y. Wu, H. Liu, P. Liu, L. Hu, Z.-F. Li and S.-Y. Liu, *ACS Appl. Polym. Mater.*, 2023, **5**, 7340–7349.
204 W. Li, H. Ma, S. Li and J. Ma, *Chem. Sci.*, 2021, **12**, 14987–15006.
205 R. Alessandri, J. J. Uusitalo, A. H. de Vries, R. W. A. Havenith and S. J. Marrink, *J. Am. Chem. Soc.*, 2017, **139**, 3697–3705.
206 L. Simine and P. J. Rossky, *J. Phys. Chem. Lett.*, 2017, **8**, 1752–1756.
207 T. Koch, J. Bachmann, T. Lettmann and N. L. Doltsinis, *Phys. Chem. Chem. Phys.*, 2021, **23**, 12233–12250.
208 D. Padula and A. Troisi, *Adv. Energy Mater.*, 2019, **9**, 1902463.
209 H. Sahu, F. Yang, X. Ye, J. Ma, W. Fang and H. Ma, *J. Mater. Chem. A*, 2019, **7**, 17480–17488.
210 N. G. An, J. Y. Kim and D. Vak, *Energy Environ. Sci.*, 2021, **14**, 3438–3446.
211 E. T. Hoke, I. T. Sachs-Quintana, M. T. Lloyd, I. Kauvar, W. R. Mateker, A. M. Nardes, C. H. Peters, N. Kopidakis and M. D. McGehee, *Adv. Energy Mater.*, 2012, **2**, 1351–1357.
212 E. M. Speller, A. J. Clarke, N. Aristidou, M. F. Wyatt, L. Francàs, G. Fish, H. Cha, H. K. H. Lee, J. Luke, A. Wadsworth, A. D. Evans, I. McCulloch, J.-S. Kim, S. A. Haque, J. R. Durrant, S. D. Dimitrov, W. C. Tsoi and Z. Li, *ACS Energy Lett.*, 2019, **4**, 846–852.
213 I. V. Martynov, L. N. Inasaridze and P. A. Troshin, *ChemSusChem*, 2022, **15**, e202101336.
214 M. A. Anderson, A. Hamstra, B. W. Larson and E. L. Ratcliff, *J. Mater. Chem. A*, 2023, **11**, 17858–17871.